American Mineralogist, Volume 97, pages 1574–1581, 2012

A multi-domain gem-grade Brazilian apatite

Tom Baikie,[1,*] Martin K. Schreyer,[2] Chui Ling Wong,[1] Stevin S. Pramana,[1] Wim T. Klooster,[3] Cristiano Ferraris,[4] Garry J. McIntyre,[3] and T.J. White[5]

[1]School of Materials Science and Engineering, Nanyang Technological University, Nanyang Avenue, 639798 Singapore
[2]Institute of Chemical Engineering Sciences, 1 Pesek Road, Jurong Island, Singapore
[3]The Bragg Institute, Australian Nuclear Science and Technology Organisation, Lucas Heights, New South Wales 2234, Australia
[4]Laboratoire de Minéralogie, USM 201, Muséum National d'Histoire Naturelle, CP 52, 61 Rue Buffon, 75005 Paris, France
[5]Centre of Advanced Microscopy, The Australian National University, Canberra ACT 0200, Australia

Abstract

A gem-grade apatite from Brazil of general composition $(Ca,Na)_{10}[(P,Si,S)O_4]_6(F,Cl,OH)_2$ has been studied using single-crystal X-ray and neutron diffraction together with synchrotron powder X-ray diffraction. Earlier electron microscopy studies had shown the nominally single-phase apatite contains an abundant fluorapatite (F-Ap) host, together with chloro-hydroxylapatites (Cl/OH-Ap) guest phases that encapsulate hydroxylellestadite (OH-El) nanocrystals. While the latter features appear as small (200–400 nm) chemically distinct regions by transmission electron microscopy, and can be identified as separate phases by synchrotron powder X-ray diffraction, these could not be detected by single-crystal X-ray and neutron analysis. The observations using neutron, X-ray and electron probes are however consistent and complementary. After refinement in the space group $P6_3/m$ the tunnel anions F^- are fixed at $z = ¼$ along <001>, while the anions Cl^- and OH^- are disordered, with the suggestion that O-H···O-H··· hydrogen-bonded chains form in localized regions, such that no net poling results. The major cations are located in the $4f\ A^FO_6$ metaprism (Ca+Na), $6h\ A^TO_6X$ tunnel site (Ca only), and $6h\ BO_4$ tetrahedron (P+Si+S). The structural intricacy of this gem stone provides further evidence that apatite microstructures display a nano-phase separation that is generally unrecognized, with the implication that such complexity may impact upon the functionality of technological analogues.

Keywords: Apatite, X-ray diffraction, Laue neutron diffraction, synchrotron X-ray diffraction

Introduction

Apatite sensu stricto has the composition $Ca_{10}(PO_4)_6(F,Cl,OH)_2$, with fluorapatite (F-Ap) (Sudarsanan et al. 1972), hydroxylapatite (OH-Ap) (Kay et al. 1964), and chlorapatite (Cl-Ap) (Mackie et al. 1972) as the designated end-members. Natural and synthetic analogues generally conform to hexagonal $P6_3/m$ symmetry and the crystal chemical formula $[A^F_4][A^T_6][(BO_4)_6]X_2$ where A includes the larger cations, B are metalloids, and X the halides or oxy-anions (White and Dong 2003). Lower-symmetry counterparts are realized through atomic ordering within, or topological adjustments of, the putative $A^F_4(BO_4)_6$ zeolite-like framework that creates $[001]_{hex}$ tunnels surrounding the $A^T_6X_2$ component (Fig. 1). The diameter of this passage adjusts through anti-symmetric rotation of alternate (001) triangular faces of A^FO_6 metaprism columns, which are corner-connected to BO_4 tetrahedra, to accommodate changes in the size or stoichiometry of the channel contents (Mercier et al. 2006; White et al. 2005). The metaprism twist angle (φ) is sensitive to the relative dimensions of the framework and tunnel constituents and when φ < 25° the apatite is hexagonal. However, for larger φ unsatisfactory bond valence sums (BVS) are resolved through $[100]_{hex}$ BO_4 rotations that reduce the symmetry to triclinic $P\bar{1}$ (Baikie et al. 2007).

Two classes of monoclinic apatites appear either as a response to X anion sub-lattice misfits ($P112_1/b$), or in chemically complex compounds, from the need to introduce multiple crystallographic sites that accept cations of disparate size and charge ($P2_1/m$ and $P2_1$). For example, OH-Ap (Hughes et al. 1989; Elliot et al. 1973) and Cl-Ap (Kim et al. 2000; Ikoma et al. 1999) are reportedly dimorphic, adopting both hexagonal $P6_3/m$ and monoclinic $P112_1/b$ structures, although small compositional departures from $Ca_{10}(PO_4)_6(OH)_2$ and $Ca_{10}(PO_4)_6Cl_2$ may be a pre-requisite for the stabilization of those monoclinic forms. Nonetheless, it is clear that anti-parallel <001> offsets of the OH/Cl atoms along the tunnels are essential to avoid over-bonding (Le Page and Rodgers 2005) and these displacements destroy the mirror symmetry in $P6_3/m$ and lead to a doubling along one a_{hex} axis.

Compositionally intricate natural apatites show a wide range of coupled ionic substitutions combined with various degrees of non-stoichiometry (Pan and Fleet 2002) that are facilitated through the crystallization of lower-symmetry analogues conforming to maximal non-isomorphic space groups of $P6_3/m$ (White and Dong 2003). A typical representative is ellestadite (El-Ap), where the $2P^{5+} \leftrightarrow Si^{4+}+S^{6+}$ substitution leads to a monoclinic $P2_1$ structure idealized as $[Ca_4][Ca_6][(PO_4)_{1-2x}(SiO_4)_x(SO_4)_x]_6(F,Cl,OH)_2$ (Organova et al. 1994). Beyond chemically induced symmetry modification, complex apatite nanostructures have been observed in synthetic materials that depart from thermodynamic equilibrium such as $[Ca,Pb]_{10}([V,P]O_4)_6(F,O)_{2-x}$ (Dong and White 2004a, 2004b), or in equilibrated minerals, where it has been proposed that spinodal decomposition and phase separation take place (Ferraris et al. 2005).

* E-mail: tbaikie@ntu.edu.sg

0003-004X/12/0010–1574$05.00/DOI: http://dx.doi.org/10.2138/am.2012.4069

In an earlier study, it was shown by conventional powder X-ray diffraction and transmission electron microscopy that gem-grade apatite from Brazil (Fig. 2) consists of host F-Ap (~450 nm domains) surrounding guest OH/Cl-Ap domains (~250 nm) that, in turn, encapsulate faceted nano-sized hydroxylellestadite (OH-El) crystals. The F-Ap and OH/Cl-Ap were described as hexagonal $P6_3/m$ while OH-El was assigned as monoclinic $P2_1/m$ symmetry (Ferraris et al. 2005) (Fig. 3). However, as symmetry

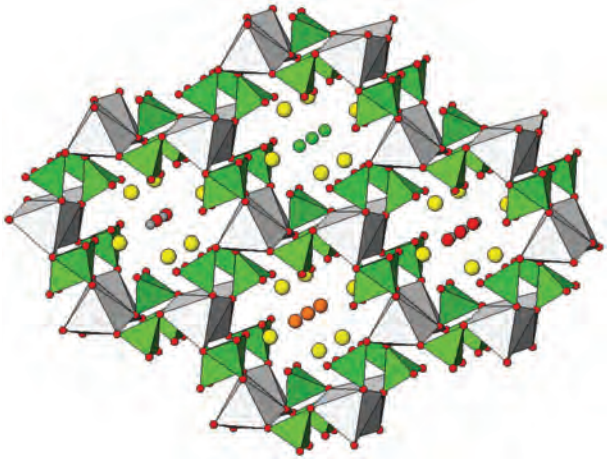

FIGURE 1. A schematic illustration of the framework motif and types of tunnel-anion order found in Brazilian apatite gems. The gray AO_6 polyhedra are metaprisms containing calcium and sodium, while the green BO_4 tetrahedra accommodate phosphorus, silicon, and sulfur. The tunnels contain calcium (yellow) and the tunnel anions fluorine (green), chlorine (orange), and hydroxyl (oxygen red, hydrogen gray) in two orientations. (ATOMS, Dowty 2002).

FIGURE 2. The apatite crystal used for the neutron diffraction experiment.

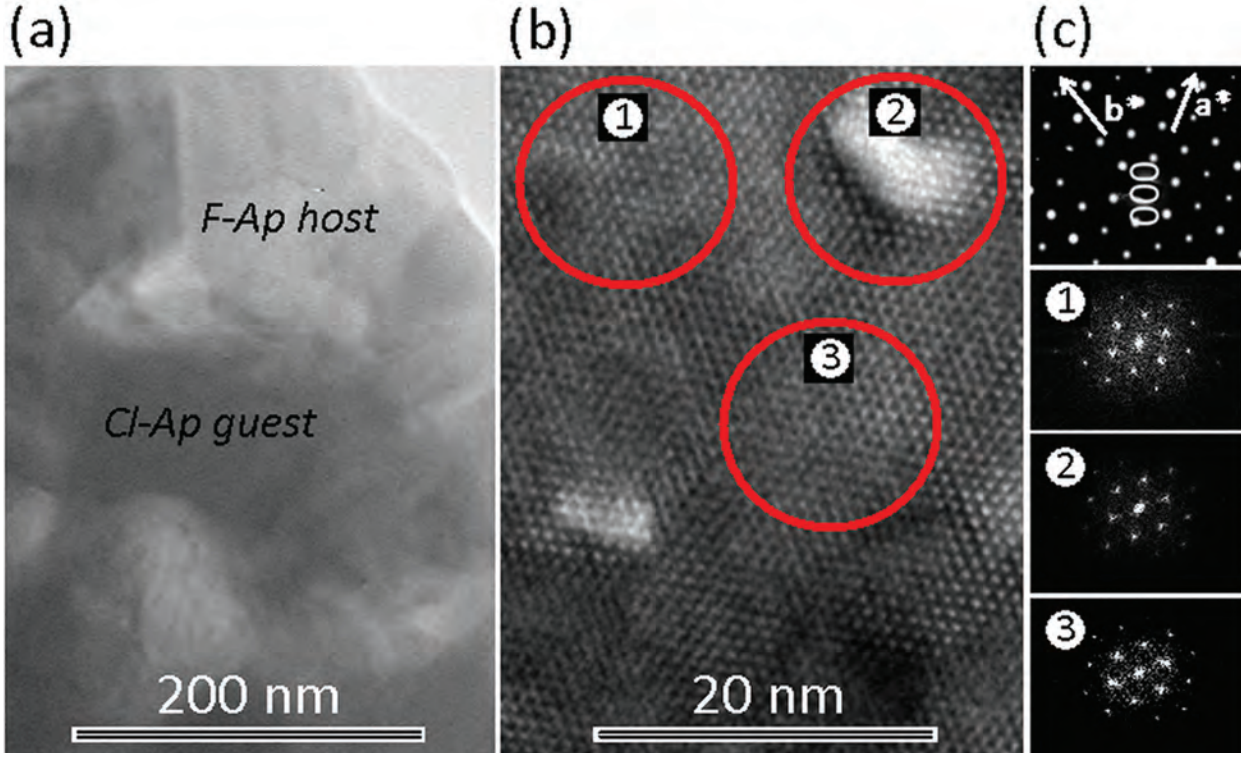

FIGURE 3. Transmission electron microscopy (**a**) a [001] bright-field image containing the F-Ap host (lighter contrast) and Cl-Ap guest apatite (dark contrast); (**b**) the [001] high-resolution image where ellestadite nanodomains, richer in Na+Si+S, are embedded in host and guest apatites. (**c**) Uppermost the pattern obtained from a crystal volume containing the region shown in **a** is given. FFT were collected from (1) an ellestadite region, (2) an electron-beam damaged region, and (3) a guest region. Small changes on orientation are evident. Elsewhere, energy-dispersive X-ray microanalysis has been used to confirm the compositional uniqueness of these regions (Ferraris et al. 2005).

reduction arising from light elements (especially the tunnel anions) could not be addressed, and some phase domains were electron-beam sensitive, supplementary single-crystal X-ray and neutron diffraction experiments, combined with synchrotron powder X-ray diffraction are reported here to verify and extend the conclusions drawn from the previous work.

The examination of multiphase "single" crystals by either X-ray or neutron diffraction is rarely attempted, in part because such materials would normally be considered inferior specimens. However, such analyses are feasible, as in the case of the co-determination of the structures of zirconolite and zirkelite crystals that were too small to separate into phase-pure grains (Mazzi and Munno 1983). The current study, while being more ambitious with four apatites considered simultaneously is possible because the chemically distinct regions are texturally coherent, or almost so. In addition, the space-group relationships between apatites are well understood.

Experimental methods

EPMA and TEM

In Ferraris et al. (2005), the composition of the apatite collected from Ipirá, Bahia Province, Brazil, was determined by electron microprobe analysis (EPMA) to be $(Ca_{3.95}Na_{0.05})Ca_{5.99}(P_{5.69}Si_{0.18}S_{0.13})O_{24}(F_{1.52}Cl_{0.12}OH_{0.36})$. The EPMA of apatite is analytically challenging (McCubbin et al. 2010; Pyle et al. 2002; Stormer et al. 1993) and the chemical composition determined in the previous study was obtained without any constraint to the overall charged balancing. Specifically, because EPMA cannot be used to determine OH, the 0.36 structural formula units (sfu) of hydroxyl were derived on the assumption that the channel ions sum to 2 per unit cell, i.e., F+Cl+OH = 2. McCubbin et al. (2010) determined that a missing structural component in the monovalent channel ion site of apatite must be greater than 0.16 sfu before it is above the minimum threshold for detection. The missing component of 0.36 sfu found in Ferraris et al. (2005) exceeds this minimum threshold for detection. In addition to the expected channel species found, Pan and Fleet (2002) noted that the apatite X-site can hold any number of anions including CO_3^{2-}, Br^-, I^-, S^{2-}, O^{2-} as well structural vacancies and electroneutral molecules such as H_2O; however, these were not detected in the previous study. Transmission electron microscopy (TEM) investigations were carried out on ion-milled crystallographically oriented slices. Sample and technical details for the TEM and EPMA are available in Ferraris et al. (2005).

Synchrotron powder X-ray diffraction (SPXRD)

Synchrotron powder X-ray diffraction data were collected using the X-ray Development and Demonstration Beamline of the Singapore Synchrotron Light Source that operates a Helios 2 storage ring at 700 MeV with a typical stored beam current of 300 mA. X-ray energy was selected with a Si (111) channel-cut monochromator blocked to be 1 mm high vertically and focused to a horizontal width of 3.5 mm by the collimating mirror and slit system. The configuration yielded an X-ray beam of 0.01° divergence at 8.048 keV. The detector slit was adjusted to be 1 mm high. The diffractometer was the Huber 4-circle system 90000-0216/0, with high-precision 0.0001° step size for the omega and two-θ circles using Bragg-Brentano geometry. The distance from entrance slit to sample was 688 mm and from sample center to detector 680 mm. The sample was gently pressed into a flat-plate sample holder in an attempt to reduce preferred orientation. To maximize the incident and diffracted X-ray intensities most of the beam path was encapsulated in a plastic tube filled with helium gas. However, the sample itself was exposed to air. The data were collected using a step size of 0.02° with a counting time of 5 s per data point, which defined the FWHM of each reflection by at least 5 data points. All samples were scanned over the range 15–140° in 2θ. Prior to analysis the raw data were normalized to the counts recorded by the incident-beam monitor. The data were analyzed using TOPAS V4.1 (Bruker 2008).

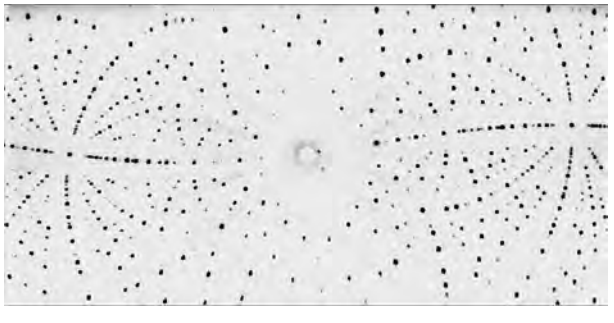

Figure 4. Laue diffraction pattern collected at VIVALDI, ILL.

Single-crystal neutron data collection

Neutron diffraction data were gathered from a euhedral blue crystal (Fig. 2) on the Very Intense Vertical Alignment Laue Diffractometer (VIVALDI) at the Institut Laue-Langevin (ILL), Grenoble, France. VIVALDI uses Laue diffraction on a polychromatic thermal-neutron beam coupled with a large solid-angle (eight steradians) cylindrical image-plate detector, to increase the detection efficiency of the sum of diffracted intensities by one to two orders of magnitude compared with a conventional monochromatic experiment (McIntyre et al. 2006; Wilkinson et al. 2002). The apatite crystal of approximate dimensions 6 × 5 × 4 mm was wrapped in aluminum foil smeared with silicone grease and glued to a vanadium pin, then mounted in a helium-flow cryostat and cooled to 130 K. Five Laue diffraction patterns were collected at 20° intervals around the vertical axis perpendicular to the incident neutron beam, with each exposure lasting just 5 min (Fig. 4). The sample volume is considerably larger than the 1 mm^3, which is typical for structural studies on VIVALDI, but a further goal of this neutron study was to demonstrate that a sensible structural refinement could be obtained from such a large sample. The large volume dictated in turn very short exposure times to avoid individual pixel counts in the recorded Laue patterns exceeding the maximum possible of 65 535.

The diffraction patterns were indexed using the program LAUEGEN (Campbell 1995; Campbell et al. 1998) and the reflections integrated using a 2D version of the $\sigma(I)/I$ algorithm described by Wilkinson et al. (1988) and Prince et al. (1997). No absorption correction was necessary (μ = 0.038 cm^{-1}). The short exposure time necessitated a correction for the decay of 2.5% of the latent image during the 3.5 min readout. Correction was also made for the higher probability of neutron capture away from the equatorial plane by the ^{158}Gd found in natural abundance in the Gd_2O_3 scintillator of the image plate (R.O. Piltz, personal communication). The reflections were then normalized to a common incident wavelength, using a curve derived by comparing equivalent reflections and multiple observations, via the program LAUENORM (Campbell et al. 1986). Only reflections with wavelengths between 1.0 and 2.9 Å were accepted for the normalization procedure, as those outside this range were too weak, or had too few equivalents to allow determination

Table 1. Crystallographic data and refinement parameters from the single-crystal X-ray and neutron diffraction data

Formula	$A_{10}B_6O_{24}F_{1.428}(OH)_{0.696}$* Neutron	$A_{10}B_6O_{24}F_{1.46}O_{0.54}$ X-ray
T (K)	130	100
Wavelength (Å)	1.0 ≤ λ ≤ 2.9	0.71073
Crystal system	Hexagonal	Hexagonal
Space group	$P6_3/m$	$P6_3/m$
Unit-cell dimensions:		
a (Å)	9.3687†	9.3687(2)
c (Å)	6.8739†	6.8739(1)
V (Å^3)	522.51(1)	522.51(1)
Z	2	2
D_c (g/cm^{-3})	3.176	3.2044
μ, cm^{-1}	0.038	3.106
Reflections collected	2426	8078
Independent Reflections. (R_{int})	414 (0.0046)	551
Data/restraints/parameters	408/0/42	542/0/41
***R* indices (all data):**		
$R(F^2)$	0.0554	0.0198
$wR(F^2)$	0.0605	0.0642
GoF (F^2)	1.128	1.56
R indices [$I > 3\sigma(I)$]		
$R(F^2)$	0.0515	0.0200
$wR(F^2)$	0.0599	0.0643
GoF (F^2)	1.163	1.58

* *A* = Ca + Na; *B* = P + Si +S.
† The absolute scale of the unit-cell lengths cannot be determined in the white beam Laue method; *c* was fixed at the X-ray value.

of the normalization curve confidently. The total number of observed reflections accepted was 2426, which were averaged to give 414 unique reflections (R_{int} = 0.0046), of which 384 have $F^2 > 3\sigma(F^2)$. The resulting intensities were used in a full-matrix least-squares refinement using UPALS (Lundgren 1982). An isotropic type I extinction correction was applied (Becker and Coppens 1974). In the final refinement, the scale factor and the positional and anisotropic atomic displacement parameters for all atoms were refined, except for F, Cl, and OH that were treated isotropically to give a total of 42 variables. The value of the goodness-of-fit is close to 1.0, indicating that a lower *R* factor cannot be expected. A summary of the crystal, data-collection, and refinement parameters is given in Table 1. The neutron scattering lengths of 0.4700, 0.5130, 0.5803, 0.5654, –0.37390, and 0.9577 $\times 10^{-12}$ cm were used for Ca, P, O, F, H, and Cl, respectively (Sears 1993).

Single-crystal X-ray data collection

A small fragment (0.1 × 0.1 × 0.1 mm) was cleaved from the large crystal used in the neutron diffraction study. Data were collected on a Bruker Smart Apex II three-circle diffractometer at 100 K using Mo$K\alpha$ radiation with a graphite monochromator over the angular range 2.5 to 30.5 °2θ. A total of 542 reflections with $I > 3\sigma(I)$ were collected and the structures refined using Jana 2006 (Petříček et al. 2006) utilizing the Superflip (Palatinus and Chapuis 2007) structure-solution algorithm. (CIF[1] is on deposit.)

Analysis strategy

In a review of reliable chemical end-member crystal-structure determinations, White and Dong (2003) found that ~60% of apatites conform to $P6_3/m$ (space group no. 176), with the remainder adopting, in decreasing order of abundance, $P6_3$ (173), $P\bar{6}$ (174), $P\bar{3}$ (147), $P2_1/m$ (11), or $P2_1$ (4) symmetry. Several space groups were tested ($P6_3/m$, $P6_3$, $P2_1/m$, and $P2_1$) with $P6_3/m$ proving superior and the statistics indicating an almost perfectly centric symmetry, but with displacement of the asymmetric hydroxyl groups and chlorine atoms. While this assignment is acceptable for F-Ap as noted before, OH/Cl cannot be located on the mirror plane as this is incompatible with bonding requirements. Therefore, in these latter cases, $P6_3/m$ is an average structure that reflects the disorder of the tunnel anion with the OH/Cl displaced off the mirror plane along <001> with equal frequency (Leroy and Bres 2001). Ellestadite is most reliably regarded as monoclinic $P2_1$ with a lattice metric close to hexagonal.

Results

Neutron diffraction data

Cell parameter refinement. Only the ratios of the linear lattice parameters can be obtained from the white-beam Laue technique. Our data gave a *c/a* ratio of 0.730, which is very close to that obtained from powder X-ray diffraction data for the host-Ap: $a = b = 9.4124(1)$ Å, $c = 6.8853(1)$ Å, $c/a = 0.7315$. [Table 1, Ferraris et al. (2005)]. There was no evident splitting or broadening of the Laue spots due to the slightly different *c*/*a* ratios of the coexisting apatite phases.

Space group selection

Several space groups were tested ($P6_3/m$, $P6_3$, $P2_1/m$, $P2_1$) with $P6_3/m$ proving superior and the statistics indicating an almost perfectly non-centric symmetry due to displacement of the asymmetric hydroxyl groups and chlorine atoms. Refinements using a monoclinic cell ($P2_1$) yielded slightly better *R*-values as compared to $P6_3/m$; however, the difference was insignificant, especially when the extra number of parameters was considered (~200 vs. 42).

Composition

According to the electron microprobe (EPMA) and selected-area electron diffraction (SAED) study of Ferraris et al. (2005) the host F-Ap accounts for ~76 wt% and the guest Cl-Ap, OH-Ap, and OH-El ~6, ~13, and ~5 wt%, respectively. The F position of fluorapatite is usually listed as 2*a* (0, 0, ¼), and a preliminary refinement of the occupancy factor of this F site gave 0.76(1) when refining isotropically, but 0.94(1) when refining anisotropically, with elongation along the **c**-axis. The 0.76 F perfectly agrees with the value obtained by EPMA. Alternatively, the 0.94 would be consistent with 0.76 F + 0.18 O, where the oxygen is associated with H as OH groups, keeping in mind that the scattering lengths of F and O are almost equal (0.5654 and 0.5803 $\times 10^{-12}$ cm, respectively). This interpretation would also be reasonable from a crystal chemical point of view: the 2*a* site, which is surrounded by a triangle of A^T cations results in over-bonding for O, which is marginally displaced along [001]. Therefore, refinement included release of the O (4*e*; 0 0 *z*) to yield a *z* coordinate of 0.316(12). This places the hydroxyl H atom at $z \sim 0.47$, assuming an O-H bond length of ~1 Å. Difference Fourier mapping confirmed the hydroxyl O near $z = 0.32$ and located the hydroxyl H around $z = 0.5$. The hydrogen can be refined at a position close to this location.

Refinements of the X-ray data showed that no crystalline Cl-Ap was present (Ferraris et al. 2005), although its cell parameters are sufficiently different to permit ready detection. This suggests that chlorine atoms, which are too large to displace F, are for the most part distributed randomly throughout the crystal, although chlorine-rich domains (~250 nm) can be located by analytical TEM. Neither did extensive difference Fourier mapping show excess scattering density attributable to Cl, which would normally appear at $z = 0.4432$ (Mackie and Young 1974). However, this location places Cl very close to the H atom, as observed in the averaged, overall structure. It was therefore unsurprising that a refinement for Cl restrained around $z = 0.4432$ failed to reveal a scattering center. A Cl positioned at (0, 0, 0) (Hendricks et al. 1932), or the equivalent (0, 0, 0.5), were similarly discounted. McCubbin et al. (2008) showed via $^{19}F(^{35}Cl)$ TRAPDOR NMR that low-OF F-Cl apatite has F and Cl mixed in the apatite channel such that all Cl ions have neighboring F atoms, and with the Cl ions positioned at $z = 0.126$. However, no scattering center was observed at this site in the current work, which is probably related to the low-Cl concentrations present in the samples studied.

While Ca is distributed over the A^F and A^T sites, the Na is expected to partition almost exclusively into the A^F framework position, as alkali ions (Na through Cs) become significantly over-bonded in the A^T site. A reconnaissance refinement that placed only Ca at the *A* sites was consistent with a small amount of Na entering the A^F. Assuming that the A^F and A^T sites are fully occupied, the scattering length for each was adjusted to give an occupancy of 1, leading to about $Na_{0.09}$ at A^F, a result not significantly different from the $Na_{0.05}$ obtained by chemical analysis. The same procedure indicated pure speciation at A^T (Ca) and O1, O2, and O3 using the standard scattering lengths (Sears 1993). A refinement of the occupancy factor of P indicates the presence of 3 wt% OH-El, assuming equimolar amounts of Si and S. This result is slightly less than the 5 wt% found by Ferraris et al. (2005). The final refined atomic positions and bond

[1] Deposit item AM-12-067, CIF. Deposit items are available two ways: For a paper copy contact the Business Office of the Mineralogical Society of America (see inside front cover of recent issue) for price information. For an electronic copy visit the MSA web site at http://www.minsocam.org, go to the *American Mineralogist* Contents, find the table of contents for the specific volume/issue wanted, and then click on the deposit link there.

TABLE 2. Fractional coordinates and displacement parameters derived from single-crystal neutron diffraction data collected at 130 K

	Wyckoff	*x*	*y*	*z*	Occ.	U_{eq}
			Fractional coordinates			
A^F*	4*f*	1/3	2/3	–0.0013(5)	0.95	0.0084(13)
A^T	6*h*	0.2438(2)	–0.0065(2)	1/4	1	0.0018(11)
B†	6*h*	0.3986(2)	0.3690(2)	1/4	1	0.0074(9)
O1	6*h*	0.3267(2)	0.4838(2)	1/4	1	0.0084(8)
O2	6*h*	0.5880(2)	0.4662(2)	1/4	1	0.0107(8)
O3	12*i*	0.3417(2)	0.2565(2)	0.0702(3)	1	0.0135(7)
F	2*a*	0	0	1/4	0.714(5)	0.0051(12)
O4	4*e*	0	0	0.316(12)	0.174(9)	0.0051
H	4*e*	0	0	0.472(6)	0.174	0.0061(15)

	U_{11}	U_{22}	U_{33}	U_{12}	U_{13}	U_{23}
			Displacement parameters			
A^F	0.0075(9)	0.0075	0.0102(35)	0.0037(5)	0	0
A^T	0.0041(10)	0.0010(10)	0.0020(31)	0.0001(8)	0	0
B	0.0070(9)	0.0099(9)	0.0054(24)	0.0056(7)	0	0
O1	0.0122(8)	0.0087(8)	0.0044(20)	0.0068(7)	0	0
O2	0.0055(7)	0.0099(8)	0.0165(21)	0.0032(6)	0	0
O3	0.0187(7)	0.0106(6)	0.0112(19)	0.0099(5)	–0.0059(7)	–0.0025(7)

* *A* = Ca + Na.
† *B* = P +Si + S.

TABLE 3. Selected distances (Å) and bond valence sums for BO_4, A^FO_6, and A^TO_6 from single-crystal neutron and X-ray diffraction data

Bond	Distance (neutron)	Distance (XRD)
A^F-O1 × 3	2.412(3)	2.3963(9)
A^F-O2 × 3	2.436(3)	2.4466(13)
A^F-O3 × 3	2.796(3)	2.7951(11)
A^T-O1 × 1	2.687(3)	2.6813(17)
A^T-O2 × 1	2.358(2)	2.3663(14)
A^T-O3 × 4	2.343(2), 2.486(2)	2.3436(10), 2.4896(10)
A^T-F × 1	2.315(2)	2.3104(5)
A^T-O4	2.359 (20)	2.3409(4)
B-O1 × 1	1.528(2)	1.5346(19)
B-O2 × 1	1.540(3)	1.5372(14)
B-O3 × 2	1.537(2)	1.5364(9)
O4-H	1.07(4)	–
BO_4	4.90(P^{5+} + Si^{4+} + S^{6+})	4.93
A^FO_6	1.72 (Ca^{2+} + Na^{+})	1.73
A^TO_6	2.01 (incl. 2 OH^-)	2.07

lengths are given in Tables 2 and 3 and the final refined structure is shown in Figure 5.

Single-crystal X-ray diffraction

The refinement of single-crystal X-ray diffraction data gave essentially the same results as the neutron diffraction study but with an apparent improvement on the precision of the atomic positions and bond lengths (Tables 3 and 4). When only F was placed in the channel, the refinement gave this site as ~92% occupied with a large anisotropic atomic displacement parameter (ADP) along the channel ($U_{33} \approx 0.06$). Using a similar protocol to the neutron refinement an O atom was placed at a 4*e* Wyckoff position 0, 0, *z* ($z \approx 0.32$), with the ADP values for F and O refined isotropically and with their overall occupancy summed to unity. There was little difference in the reliability indices between a refinement including an F position with anisotropic displacement parameters or split positions with O and F. This is unsurprising as X-rays are interacting with a diffuse electron cloud rather than the point scattering achieved with neutrons. Similar to the neutron diffraction study, extensive Fourier mapping was carried out and a weak (~0.5 electrons) and diffuse scattering volume was found close to 0, 0, 0. Both H and Cl atoms were separately included into the refinement and yielded relative occupancies

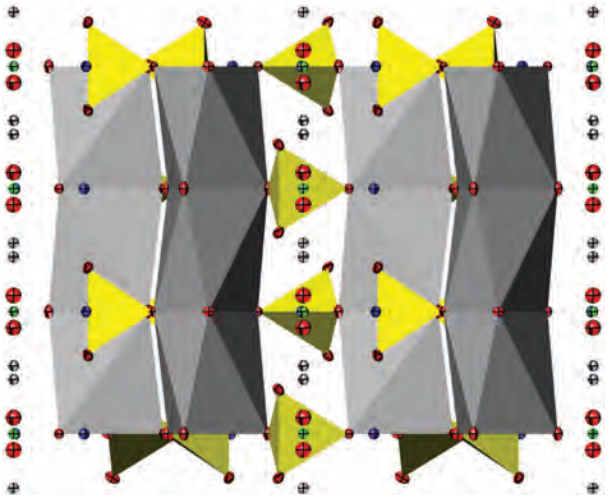

FIGURE 5. Structural representation of the Brazilian apatite derived from the single-crystal neutron diffraction refinement. The red, green, and gray ellipsoids represent the oxygen, fluorine, and hydrogen atoms, respectively.

TABLE 4. Fractional coordinates and displacement parameters derived from single-crystal X-ray diffraction data collected at 100 K

	Wyckoff	*x*	*y*	*z*	Occ.	U_{eq}
			Fractional coordinates			
A^F*	4*f*	1/3	2/3	0.00111(5)	0.98	0.00776(16)
A^T	6*h*	0.24293(4)	–0.00716(4)	1/4	1	0.00724(18)
B†	6*h*	0.39852(6)	0.36890(6)	1/4	1	0.0057(2)
O1	6*h*	0.32624(18)	0.48413(15)	1/4	1	0.0081(5)
O2	6*h*	0.58796(17)	0.46605(16)	1/4	1	0.0109(5)
O3	12*i*	0.34215(13)	0.25650(10)	0.07012(12)	1	0.0129(4)
F	2*a*	0	0	1/4	0.730(10)	0.0101(8)
O4	4e	0	0	0.305(3)	0.135(5)	0.0101(8)

	U_{11}	U_{22}	U_{33}	U_{12}	U_{13}	U_{23}
			Displacement parameters			
A^F	0.0091(2)	0.0091(2)	0.0051(3)	0.00454(10)	0	0
A^T	0.0080(3)	0.0066(2)	0.0070(3)	0.00355(15)	0	0
B	0.0066(3)	0.0058(3)	0.0056(3)	0.00381(19)	0	0
O1	0.0099(7)	0.0072(6)	0.0092(6)	0.0057(5)	0	0
O2	0.0069(6)	0.0084(7)	0.0171(6)	0.0037(5)	0	0
O3	0.0216(5)	0.0110(5)	0.0094(4)	0.0106(4)	–0.0064(4)	–0.0035(3)

* *A* = Ca + Na.
† *B* = P +Si + S.

of ~0.6 H or 0.02 Cl (with the isotropic ADP fixed at U_{iso} = 0.02). The additions of H or Cl to the apatite channel offered a slight improvement to the refinement indices but as X-rays are generally insensitive to hydrogen, the small differences may be considered insignificant. The occupancy of the A^F site refined as slightly less than unity (98% occupancy), confirming a limited incorporation of Na at this site.

Synchrotron powder X-ray diffraction (SPXRD)

The previous conventional powder X-ray diffraction study of the Brazilian apatite (Ferraris et al. 2005) noted that the *hk*0 reflections were broader than the 00*l* reflections suggesting the presence of separate apatite phases. However, the resolution of the experiment was insufficient for the separation of anisotropic reflections into individual phases. Therefore data were collected on the same sample using monochromatic synchrotron radiation.

Preferred orientation was observed because a relatively

coarse, manually ground powder was used. As a consequence, only a finite number of diffracting crystallites were illuminated by the beam resulting in a non-random distribution of orientations. To avoid textured effects, a micronizing mill (McCrone, U.K.) was employed; however this procedure also removed reflection anisotropy/splitting, suggesting the micronization was modifying the sample composition. This is not unexpected as recent work has shown that lanthanum silicate apatite electrolytes can be synthesized at room temperature by mechanically milling the constituent oxides La_2O_3 and SiO_2 (Fuentes et al. 2006). However, the objective of this experiment was to determine whether distinct apatite phases could be identified, therefore a Pawley fit of the data was performed to extract their lattice parameters. A three-phase fit containing two hexagonal phases and a monoclinic ellestadite-type phase, as identified by electron microscopy is shown in Figure 6 and clearly validates anisotropic reflection broadening and peak splitting. A Pawley fit containing three hexagonal phases was also attempted; however, the reliability indices and profile fit indicated the former was the preferred choice. The R_{wp} from the three-phase fitting (21.0%) offered a significant improvement to a two-phase fit (28.9%), and the considerably higher single phase fit (35.8%). The lattice parameters for the two hexagonal apatite phases are in good agreement with those expected for F-Ap [a = 9.4246(4), c = 6.8816(2) Å] and OH-Ap [a = 9.4118(2), c = 6.8855(3) Å], and these, together with the refined lattice parameters of ellestadite-type phase [a = 9.4122(3), b = 9.3999(1), c = 6.8940(2) Å, γ = 119.877(3)°, in space group $P112_1/m$] are comparable to values determined from electron diffraction (Ferraris et al. 2005). In addition, the refined data agree with earlier electron microscopy and conventional powder X-ray diffraction experiments that noted there was a greater variation in the a parameter as a function of composition.

Discussion

This refinement of the individual components of a multi-domain single crystal is essentially complementary to the data obtained by electron microscopy with the single-crystal experiments providing an average model of the crystal chemistry, with the powder experiment revealing phase separation into chemically distinct domains. Agreement between the techniques provides a high level of confidence that the description of this Brazilian apatite is essentially complete. Analysis of the single-crystal X-ray and neutron diffraction patterns was possible because all the apatite domains, F-Ap, OH-Ap, Cl-Ap, and OH-El, were topotaxic, and within the resolution of the experimental techniques, the diffracted intensity of individual reflections was the sum of contributions from each phase. Nonetheless, small differences in cell parameters ($9.39 < a < 9.43$ Å and $6.88 < c < 6.90$ Å) are present, as shown by synchrotron powder X-ray diffraction experiments. High-resolution electron microscope images found that local strain preserves the coherency of adjacent domains (Ferraris et al. 2005). However, the mismatch is minimal as the Laue images give no indication of diffuse scattering. While the location of F at 2a (0 0 ¼) within the A^T triangle is consistent with earlier studies (Sudarsanan et al. 1972), Cl is usually reported at 4e (0 0 z), with z in the range of 0.3–0.4 (Mackie et al. 1972). The bond-valence sum (BVS) for Cl at (0, 0, 0.25) is 3.4, and evidently unsatisfactory, while a somewhat better location at z = (0, 0, 0.4432), gives a BVS of 1.71. The best value of 1.47 was obtained with Cl at (0, 0, 0.5), but this remains unacceptably large and shows the lattice is F dominant. In the reported Cl-Ap structure the BVS is 1.05, very close to the expected value of 1. In this structure, the Cl···Ca distance is slightly larger than found in F-Ap and OH-Ap. The

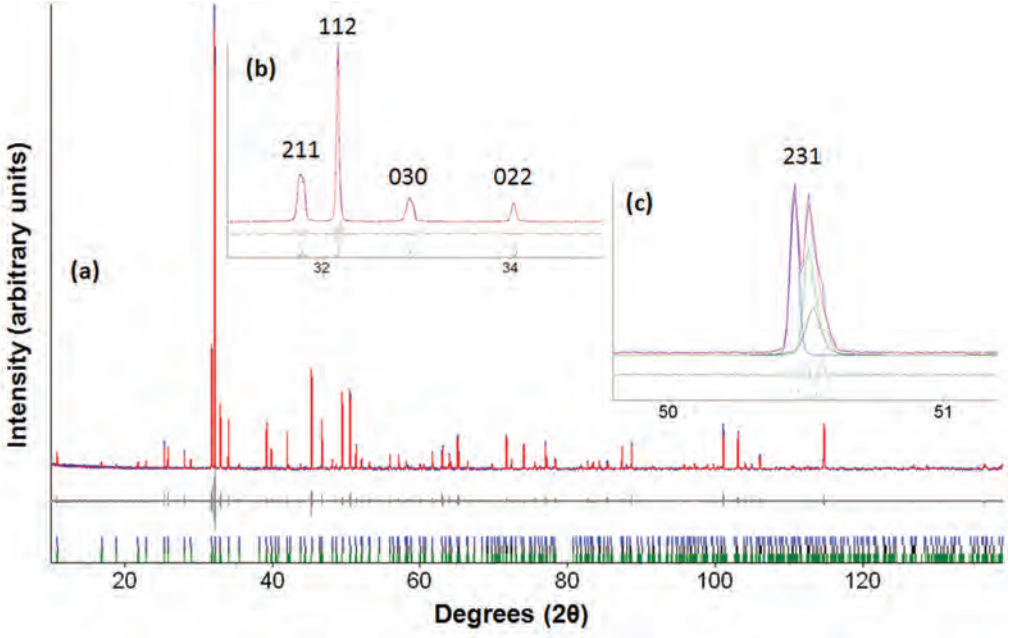

Figure 6. Pawley fit of the synchrotron data for the Brazilian apatite: (**a**) whole pattern; (**b**) selected region of the low-angle data showing reflections broadening and partial splitting; (**c**) selected region of the high-angle data showing a clear splitting of reflections and the requirement of three phases to fit the data.

partitioning of Na^+ to the A^F site and equimolar substitutions of $Si^{4+}+S^{6+}$ to the B site are explicable in terms of ionic size and charge. The BVS for the refined proportions of P+Si+S in BO_4 is 4.90, close to the expected value of 5 (Table 4). The BVS for Ca in A^FO_4 is 1.72 and slightly lower than the formal valence due to the minor substitution of Ca by Na, while A^TO_6X yields 2.01 that is consistent with full occupancy by Ca. An outstanding matter is the question of the true symmetry of the ellestadite component. While natural ellestadite is apparently monoclinic, a recent investigation of synthetic $Ca_{10-y}(SiO_4)_3(SO_4)_3Cl_{2-x-2y}F_x$ found $P6_3/m$ as the best crystallographic model across the series (Fang et al. 2011). At present, the data concerning this mineral is rather limited and further work is needed to establish the extent of Si^{4+}/S^{6+} and Na^+ substitution for P^{5+} and Ca^{2+}, respectively, required to promote lattice distortion.

It can be concluded that the Brazilian apatite contains four phase types. The tunnel anions F are at fixed special positions along <001>, while the anions Cl and OH are displaced in a disordered fashion, with the suggestion that O-H···O-H··· hydrogen-bonded chains form in localized regions, such that balanced antisymmetric ordering avoids poling. The A^FO_6 metaprism twist angle of 23.4° for the average structure is consistent with previously reported values for the end-members (F-Ap = 23.3°; OH-Ap = 23.2°; Cl-Ap = 19.1°) and confirms that the chlorine component is relatively insignificant.

From the geological and petrological view point, the nanostructure of the Ipirà apatite "single" crystals possibly arises from consecutive, or nested, spinodal decompositions. The amplitudes of the compositional modulations are assumed constant, with long wavelength (about 400–500 nm) separation of host F-Ap, and guest OH-Ap and Cl-Ap arising from the bulk composition. Before, during or after this long wave event, decomposition of higher frequency (about 10 nm) lead to the formation of OH-El. This combination of periodicities suggests that the Ipirà apatite experienced at least two significant geothermometric events.

A first long period modulation would have developed close to the coherent spinodal decomposition temperature resulting in the separation of X anions primarily and the formation of fluorine-rich and chlorine rich apatites. This kinetically driven phase separation is interpreted to coincide with the geological age (El-Rey Silva et al. 1996) of the host rocks. The higher frequency modulation possibly occurred as a result of a short time episode at slightly higher temperatures (contact metamorphism) during late intrusion of basic bodies (El-Rey Silva et al. 1996), was diffusion-dependent, and resulted in the formation of smaller ellestadite domains. If this later event was above the coherent spinodal decomposition temperature, exsolution of OH-El by homogeneous nucleation may be the preferred mechanism.

The unexpected coexistence of multiple phases in this apatite gem stone illustrates the complexity of this intriguing structural family and the need to examine these materials using probes of complementary sensitivity and resolution. It seems probable that natural and synthetic apatites may exhibit composite microstructures and lower symmetry than presently recognized. Such features may prove important when optimizing the functionality of apatites designed as heterogeneous catalysts and solid electrolytes. This study has also demonstrated that highly credible structural data can be obtained very rapidly by modern neutron Laue diffraction from large single crystals, to give a bulk averaging over the phases in a non-destructive manner.

Acknowledgments

This work was supported by MOE Tier 2 and A*Star PSF Grant numbers T208B1212 and 082 101 0021, respectively. Crystals were generously provided by our Brazilian colleague R. Wegner (Departamento de Mineração e Geologia, Campus II UFPb, CP 10094 58.109-970, Campina Grande Pb, Brazil).

References cited

Baikie, T., Mercier, P.H.J., Elcombe, M.M., Kim, J.Y., Page, Y.L., Mitchell, L.D., and White, T.J. (2007) Triclinic apatites. Acta Crystallographica, B63, 251–256.

Becker, P.J. and Coppens, P. (1974) Extinction within the limit of validity of the Darwin transfer equations. I. General formalisms for primary and secondary extinction and their application to spherical crystals. Acta. Crystallographica, A30, 129–147.

Bruker (2008) Topas Version 4.1. Bruker AXS Inc., Madison, Wisconsin, U.S.A.

Campbell, J.W. (1995) LAUEGEN, an X-windows-based program for the processing of Laue X-ray diffraction data. Journal of Applied Crystallography, 28, 228–236.

Campbell, J.W., Habash, J., Helliwell, J.R., and Moffat, K. (1986) Information quarterly for Protein Crystallogr. No. 18, SERC Daresbury Laboratory, Warrington, England, 23.

Campbell, J.W., Hao, Q., Harding, M.M., Nguti, N.D., and Wilkinson, C. (1998) Laugen version 6.0 and INTLDM. Journal of Applied Crystallography, 31, 496–502.

Dong, Z. and White, T.J. (2004a) Calcium-lead fluoro-vanadinite apatites. I Disequilibrium structures. Acta Crystallographica, B60, 138–145.

——— (2004b) Calcium-lead fluoro-vanadinite apatites. II. Equilbrium structures. Acta Crystallographica, B60, 146–154.

Dowty, E. (2002) ATOMS, Version 6.0. Shape Software, Kingsport, Tennessee.

Elliot, J.C., Mackie, P.E., and Young, R.A. (1973) Monoclinic hydroxyapatite. Science, 180, 1055–1057.

El-Rey Silva, L.J.H., Oliveira, J.G., and Gaal, E.G. (1996) Implication of the Caraiba deposits structural controls on the emplacement of the Cu-bearing hypersthenites of the Curaça valley, Bahia-Brazil. Revista Brasileira de Geociências, 26, 181–196.

Fang, Y., Ritter, C., and White, T. (2011) The crystal chemistry of $Ca_{10-y}(SiO_4)_3(SO_4)_3Cl_{2-x-2y}F_x$ ellestadite. Inorganic Chemistry, 50, 12641–12650.

Ferraris, C., White, T.J., Plevert, J., and Wegner, R. (2005) Nanometric modulation in apatite. Physical Chemistry of Minerals, 32, 485–492.

Fuentes, A.F., Rodríguez-Reyna, E., Martínez-González, L.G., Maczka, M., Hanuza, J., and Amador, U. (2006) Room-temperature synthesis of apatite-type lanthanum silicates by mechanically milling constitutent oxides. Solid State Ionics, 177, 1869–1873.

Hendricks, S.B., Jefferson, M.E., and Mosley, V.M. (1932) The crystal structures of some natural and synthetic apatite-like substances. Zeitschrift für Kristallographie, 81, 352–369.

Hughes, J.M., Cameron, M., and Crowley, K.D. (1989) Structural variations in natural F, OH and Cl apatites. American Mineralogist, 74, 870–876.

Ikoma, T., Yamazaki, A., Nakamura, S., and Akao, M. (1999) Preparation and structure refinement of monoclinic hydroxyapatite. Journal of Solid State Chemistry, 144, 272–276.

Kay, M.I., Young, R.A., and Posner, A.S. (1964) Crystal structure of hydroxyapatite. Nature, 204, 1050–1052.

Kim, J.Y., Fenton, R.R., Hunter, B.A., and Kennedy, B.J. (2000) Powder diffraction studies of calcium and lead apatites. Australian Journal of Chemistry, 53, 679–686.

Le Page, Y. and Rodgers, J.R. (2005) Quantum software interfaced with crystal-structure databases: tools, results and perspectives. Journal of Applied Crystallography, 38, 697–705.

Leroy, N. and Bres, E. (2001) Structure and substitutions in fluorapatite. European Cells and Materials Journal, 2, 36–48.

Lundgren, J.O. (1982) Crystallographic Computer Programs, Report UUIC-B134-05, Institute of Chemistry, University of Uppsala, Sweden.

Mackie, P.E. and Young, R.A. (1974) Fluorine-chlorine interaction in fluorchlorapatite. Journal of Solid State Chemistry, 11, 319–329.

Mackie, P.E., Elliott, J.C., and Young, R.A. (1972) Monoclinic structure of synthetic $Ca_5(PO_4)_3Cl$, chloroapatite. Acta Crystallographica, B28, 1840–1848.

Mazzi, F. and Munno, R. (1983) Calciobetafite (new mineral of the pyrochlore group) and related minerals from Campi Flegrei, Italy: Crystal structures of polymignyte and zirkelite: Comparison with pyrochlore and zirconolite. American Mineralogist, 68, 262–276.

McCubbin, F.M., Mason, H.E., Park, H., Philips, B.L., Parise, J.B., Nekvasil, H., and Lindsley, D.H. (2008) Synthesis and characterization of low-OH-fluorchlorapatite: A single crystal XRD and NMR spectroscopic study. American Mineralogist, 93, 210–216.

McCubbin, F.M., Steele, A., Nekvasil, H., Schneiders, A., Rose, T., Fries, M., Carpenter, P.K., and Jolliff, B.L. (2010) Detection of structurally bound hydroxyl from Apollo mare basalt 15058, 128 using TOF-SIMS. American Mineralogist, 95, 1141–1150.

McIntyre, G.J., Lemée-Cailleau, M.-H., and Wilkinson, C. (2006) High-speed neutron diffraction comes of age. Physica B, 385–386, 1055–1058.

Mercier, P.H.J., Page, Y.L., Whitfield, P.S., and Mitchell, L.D. (2006) Geometrical parameterization of the crystal chemistry of $P6_3/m$ apatite. II. Precision, accuracy and numerical stability of the crystal-chemistry Rietveld refinement. Journal of Applied Crystallography, 39, 369–375.

Organova, N.I., Rastsvetaeva, R.K., Kuz'mina, O.V., Arapova, G.A., Litsarev, M.A., and Fin'ko, V.I. (1994) The crystal structure of low-symmetry ellestadite in comparison with other apatite like structures. Kristallografiya, 39, 278–282.

Palatinus, L. and Chapuis, G. (2007) Superflip – A computer program for the solution of crystal structures by charge flipping in arbitrary dimensions. Journal of Applied Crystallography, 40, 786–790.

Pan, Y. and Fleet, M.E. (2002) Composition of the apatite-group minerals: substitution mechanism and controlling factors. In M.L. Kohn, J. Rakovan, and J.M. Hughes, Eds., Phosphates Geochemical, Geobiological, and Materials Importance, 48, p. 13–49. Reviews in Mineralogy and Geochemistry, Mineralogical Society of America, Chantilly, Virginia.

Petříček, V., Dusek, M., and Palatinus, L. (2006) Jana2006. The crystallographic computing system. Institute of Physics, Praha, Czech Republic.

Prince, E., Wilkinson, C., and McIntyre, G.J. (1997) Comparison of the $\sigma(I)/I$ and least-squares methods for integration of Bragg reflections. Journal of Applied Crystallography, 30, 133–137.

Pyle, J.M., Spear, F.S., and Wark, D.A. (2002) Electron microprobe analysis of REE in apatite, monazite and xenotime: Protocols and pitfalls. Phosphates: Geochemical, Geobiological, and Materials Importance, 48, p. 337–362. Reviews in Mineralogy and Geochemistry, Mineralogical Society of America, Chantilly, Virginia.

Sears, V.F. (1993) International Tables for Crystallography. Academic Publishers, Dordrecht, Kluwer.

Stormer, J.C., Pierson, M.L., and Tacker, R.C. (1993) Variation of F-X-ray and Cl-X-ray intensity due to anisotropic diffusion in apatite during electron-microprobe analysis. American Mineralogist, 78, 641–648.

Sudarsanan, K., Mackie, P.E., and Young, R.A. (1972) Comparison of synthetic and mineral fluorapatite, $Ca_5(PO_4)_3F$, in crystallographic detail. Materials Research Bulletin, 7, 1331–1338.

White, T.J. and Dong, Z. (2003) Structural derivation and crystal chemistry of apatites. Acta Crystallographica, B59, 1–16.

White, T.J., Ferraris, C., Kim, J., and Madhavi, S. (2005) Apatite—An adaptive framework structure. In G. Ferraris and S. Merlino, Eds., Micro- and mesoporous mineral phases, 57, p. 307. Reviews in Mineralogy and Geochemistry, Mineralogical Society of America, Chantilly, Virginia.

Wilkinson, C., Khamis, H.W., Stansfield, R.F.D., and McIntyre, G.J. (1988) Integration of single-crystal reflections using area multidetectors. Journal of Applied Crystallography, 21, 471–478.

Wilkinson, C., Cowan, J.A., Myles, D.A.A., Cipriani, F., and McIntyre, G.J. (2002) VIVALDI—A Thermal-Neutron Laue Diffractometer for Physics, Chemistry and Materials Science. Neutron News, 13, 37–41.

Manuscript received December 1, 2011
Manuscript accepted May 30, 2012
Manuscript handled by Fernando Colombo

checkCIF/PLATON report

Structure factors have been supplied for datablock(s) I

No syntax errors found. CIF dictionary Interpreting this report

Datablock: I

Bond precision: P- O = 0.0013 A Wavelength=0.71069

Cell: a=9.3687(2) b=9.3687(2) c=6.8739(1)
alpha=90 beta=90 gamma=120
Temperature: 100 K

	Calculated	Reported
Volume	522.51(3)	522.51(3)
Space group	P 63/m	P 63/m
Hall group	-P 6c	-P 6c
Moiety formula	3(O4 P), 0.07(O4), 0.73(F), 5(Ca)	?
Sum formula	Ca5 F0.73 O12.27 P3	Ca5 F0.73 O12.27 P3
Mr	503.50	503.50
Dx,g cm-3	3.200	3.200
Z	2	2
Mu (mm-1)	3.107	3.106
F000	499.5	499.5
F000’	502.62	
h,k,lmax	13,13,9	12,12,9
Nref	579	551
Tmin,Tmax	0.740,0.733	0.423,1.000
Tmin’	0.726	

Correction method= MULTI-SCAN

Data completeness= 0.952 Theta(max)= 30.510

R(reflections)= 0.0198(542) wR2(reflections)= 0.0643(551)

S = 1.560 Npar= 40

The following ALERTS were generated. Each ALERT has the format
test-name_ALERT_alert-type_alert-level.
Click on the hyperlinks for more details of the test.

Alert level C
PLAT077_ALERT_4_C Unitcell contains non-integer number of atoms .. ?

Alert level G

```
PLAT005_ALERT_5_G No _iucr_refine_instructions_details in CIF ....          ?
PLAT301_ALERT_3_G Note: Main Residue  Disorder ..................        13 Perc.
```

```
   0 ALERT level A = Most likely a serious problem - resolve or explain
   0 ALERT level B = A potentially serious problem, consider carefully
   1 ALERT level C = Check. Ensure it is not caused by an omission or oversight
   2 ALERT level G = General information/check it is not something unexpected

   0 ALERT type 1 CIF construction/syntax error, inconsistent or missing data
   0 ALERT type 2 Indicator that the structure model may be wrong or deficient
   1 ALERT type 3 Indicator that the structure quality may be low
   1 ALERT type 4 Improvement, methodology, query or suggestion
   1 ALERT type 5 Informative message, check
```

It is advisable to attempt to resolve as many as possible of the alerts in all categories. Often the minor alerts point to easily fixed oversights, errors and omissions in your CIF or refinement strategy, so attention to these fine details can be worthwhile. In order to resolve some of the more serious problems it may be necessary to carry out additional measurements or structure refinements. However, the purpose of your study may justify the reported deviations and the more serious of these should normally be commented upon in the discussion or experimental section of a paper or in the "special_details" fields of the CIF. checkCIF was carefully designed to identify outliers and unusual parameters, but every test has its limitations and alerts that are not important in a particular case may appear. Conversely, the absence of alerts does not guarantee there are no aspects of the results needing attention. It is up to the individual to critically assess their own results and, if necessary, seek expert advice.

Publication of your CIF in IUCr journals

A basic structural check has been run on your CIF. These basic checks will be run on all CIFs submitted for publication in IUCr journals (*Acta Crystallographica, Journal of Applied Crystallography, Journal of Synchrotron Radiation*); however, if you intend to submit to *Acta Crystallographica Section C* or *E*, you should make sure that full publication checks are run on the final version of your CIF prior to submission.

Publication of your CIF in other journals

Please refer to the *Notes for Authors* of the relevant journal for any special instructions relating to CIF submission.

PLATON version of 18/07/2011; check.def file version of 04/07/2011

Datablock I - ellipsoid plot

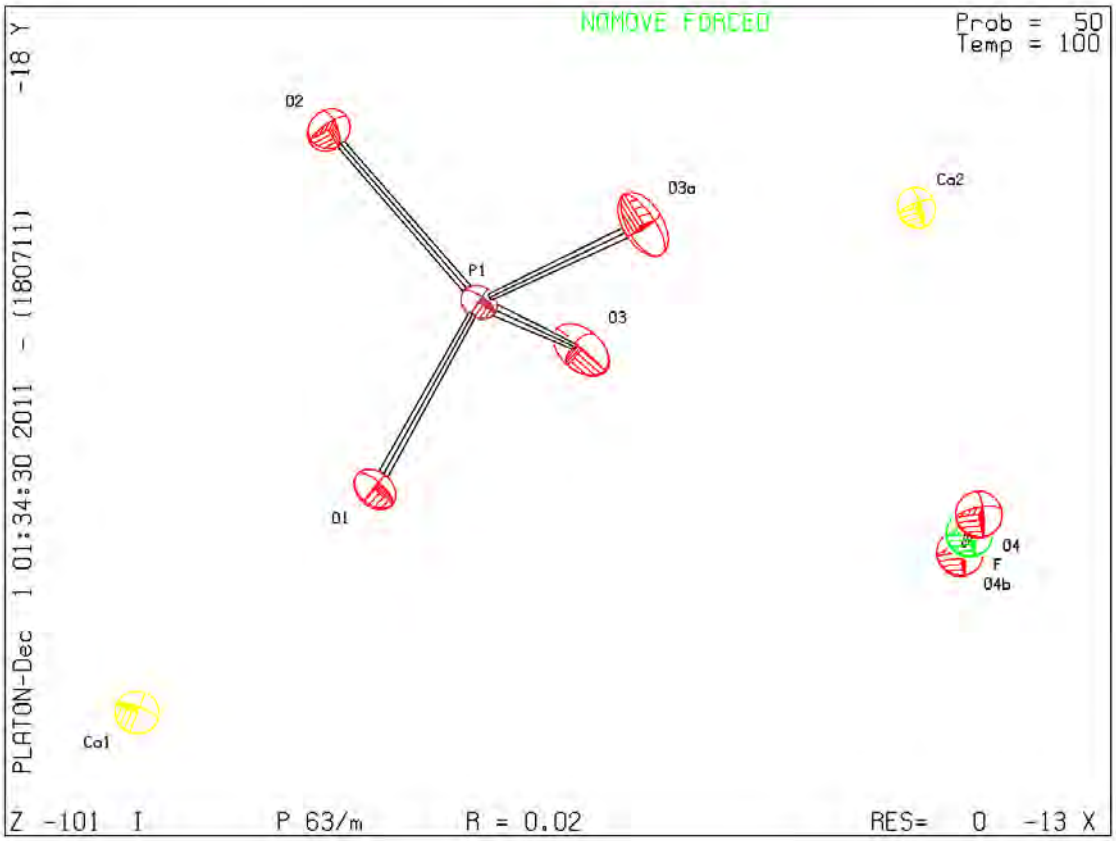

```
#======================================================================
data_global
#======================================================================

_audit_creation_method                  'Jana2006 Version : 23/10/2008'


# 1. PROCESSING SUMMARY (IUCr Office Use Only)

_journal_date_recd_electronic           ?
_journal_date_to_coeditor               ?
_journal_date_from_coeditor             ?
_journal_date_accepted                  ?
_journal_date_printers_first            ?
_journal_date_printers_final            ?
_journal_date_proofs_out                ?
_journal_date_proofs_in                 ?
_journal_coeditor_name                  ?
_journal_coeditor_code                  ?
_journal_coeditor_notes
; ?
;
_journal_techeditor_code                ?
_journal_paper_category                 ?
_journal_techeditor_notes
; ?
;
_journal_coden_ASTM                     ?
_journal_name_full                      'Acta Crystallographica Section C'
_journal_year                           ?
_journal_volume                         ?
_journal_issue                          ?
_journal_page_first                     ?
_journal_page_last                      ?
_journal_suppl_publ_number              ?
_journal_suppl_publ_pages               ?

#======================================================================

# 2. SUBMISSION DETAILS

_publ_contact_author_name               'T Baikie'
_publ_contact_author_address
; School of Materials Science and Engineering,
Nanyang Technological University,
50 Nanyang Avenue,
Singapore, 639798
;
_publ_contact_author_email              'tbaikie@ntu.edu.sg'
_publ_contact_author_fax                ?
_publ_contact_author_phone              ?

_publ_requested_journal                 'American Mineralogist'
_publ_requested_category                ?
```

```
_publ_contact_letter
; ?
;

#=============================================================================

# 3. TITLE AND AUTHOR LIST

_publ_section_title
; A Multi-Domain Brazilian Apatite Gem: Implications for Technological Materials
;
_publ_section_title_footnote
; ?
;
loop_
 _publ_author_name
 _publ_author_address
'Tom Baikie'
; Division of Materials Science & Engineering,
Nanyang Technological University, Singapore
;
'Martin Schreyer'
;Institute of Chemical Engineering Sciences (ICES),
Agency for Science, Technology and Research (A*Star), 1 Pesek Road,
Jurong Island, 627833, Singapore
;
'Chui Ling Wong'
;Division of Materials Science & Engineering,
Nanyang Technological University, Singapore
;
'Stevin S. Pramana'
;Division of Materials Science & Engineering,
Nanyang Technological University, Singapore
;
'Wim T. Klooster'
;Division of Materials Science & Engineering,
Nanyang Technological University, Singapore
;
'Cristiano Ferraris'
;Laboratoire de Mineralogie, USM 201, Museum National d'histoire naturelle,
CP 52, 61 Rue Buffon, 75005, Paris, France
;
'Garry J. McIntyre'
;The Bragg Institute, Australian Nuclear Science and Technology Organisation,
Lucas Heights, NSW 2234, Australia
;
'T. J. White'
;Electron Microscopy Unit, Australian National University,
Research School of Biology, GPO Box 475 Canberra, ACT 2601 Australia
;
#=============================================================================
data_(I)
#=============================================================================

# 4. CHEMICAL DATA
```

```
_chemical_name_systematic
; ?
;
_chemical_name_common                   ?
_chemical_formula_moiety                ?
_chemical_formula_structural            ?
_chemical_formula_analytical            ?
_chemical_formula_iupac                 ?
_chemical_formula_sum                   'Ca5 F0.73 O12.27 P3'
_chemical_formula_weight                503.50
_chemical_melting_point                 'not measured'


#==============================================================================

# 6. CRYSTAL DATA

_symmetry_cell_setting                  hexagonal
_symmetry_space_group_name_H-M          'P 63/m'
_symmetry_space_group_name_Hall         '-P 6c'
_symmetry_Int_Tables_number             176
loop_
 _symmetry_equiv_pos_site_id
 _symmetry_equiv_pos_as_xyz
 1   x,y,z
 2   -y,x-y,z
 3   -x+y,-x,z
 4   -x,-y,z+1/2
 5   y,-x+y,z+1/2
 6   x-y,x,z+1/2
 7   -x,-y,-z
 8   y,-x+y,-z
 9   x-y,x,-z
 10  x,y,-z+1/2
 11  -y,x-y,-z+1/2
 12  -x+y,-x,-z+1/2
_cell_length_a                          9.3687(2)
_cell_length_b                          9.3687(2)
_cell_length_c                          6.8739(1)
_cell_angle_alpha                       90
_cell_angle_beta                        90
_cell_angle_gamma                       120
_cell_volume                            522.51(3)
_cell_formula_units_Z                   2

_cell_measurement_reflns_used           8078
_cell_measurement_theta_min             2.51
_cell_measurement_theta_max             30.51
_cell_measurement_temperature           100
_cell_special_details
; ?
;

_exptl_crystal_density_diffrn           3.200
_exptl_crystal_density_meas             'not measured'
_exptl_crystal_density_method           'not measured'
_exptl_crystal_F_000                    499.5
```

```
_exptl_absorpt_coefficient_mu            3.106
_exptl_crystal_description               'regular'
_exptl_crystal_size_max                  0.1
_exptl_crystal_size_mid                  0.1
_exptl_crystal_size_min                  0.1
_exptl_crystal_size_rad                  ?
_exptl_crystal_colour                    'blue under sunlight'
_exptl_absorpt_correction_type           'multi-scan'
_exptl_absorpt_process_details
;'R.H. Blessing, Acta Crystallogr., Sect A 1995, 51, 33-38. '
;
_exptl_absorpt_correction_T_min          0.4226
_exptl_absorpt_correction_T_max          1

#=============================================================================

# 6. EXPERIMENTAL DATA

_exptl_special_details                   ?

_diffrn_ambient_temperature              100
_diffrn_radiation_type                   'Mo K\a'
_diffrn_radiation_source                 'X-ray tube'
_diffrn_radiation_wavelength             0.71069
_diffrn_radiation_monochromator          graphite
_diffrn_measurement_device               'three-circle diffractometer'
_diffrn_measurement_device_type          'Bruker CCD'
_diffrn_detector_area_resol_mean         ?
_diffrn_measurement_method               \w/2\q

_diffrn_reflns_number                    8078
_diffrn_reflns_theta_min                 2.51
_diffrn_reflns_theta_max                 30.51
_diffrn_reflns_theta_full                30
_diffrn_measured_fraction_theta_max      0.94
_diffrn_measured_fraction_theta_full     0.98
_diffrn_reflns_av_R_equivalents          0.0296
_diffrn_reflns_av_sigmaI/netI            0.0107
_diffrn_reflns_limit_h_min               -12
_diffrn_reflns_limit_h_max               11
_diffrn_reflns_limit_k_min               -11
_diffrn_reflns_limit_k_max               12
_diffrn_reflns_limit_l_min               -9
_diffrn_reflns_limit_l_max               9
_diffrn_reflns_reduction_process         ?

_diffrn_standards_number                 ?
_diffrn_standards_interval_count         ?
_diffrn_standards_interval_time          ?
_diffrn_standards_decay_%                ?
loop_
_diffrn_standard_refln_index_h
_diffrn_standard_refln_index_k
_diffrn_standard_refln_index_l
  ? ? ?
```

```
#=============================================================================

# 7. REFINEMENT DATA

_refine_special_details
; ?
;

_reflns_number_total                    551
_reflns_number_gt                       542
_reflns_threshold_expression            'I>3\s(I)'

_refine_ls_structure_factor_coef        Fsqd
_refine_ls_R_factor_gt                  0.0198
_refine_ls_wR_factor_gt                 0.0642
_refine_ls_R_factor_all                 0.0200
_refine_ls_wR_factor_ref                0.0643
_refine_ls_goodness_of_fit_ref          1.56
_refine_ls_goodness_of_fit_gt           1.57
_refine_ls_restrained_S_gt              ?
_refine_ls_restrained_S_all             ?
_refine_ls_number_reflns                551
_refine_ls_number_parameters            40
_refine_ls_number_restraints            0
_refine_ls_number_constraints           0
_refine_ls_weighting_scheme             sigma
_refine_ls_weighting_details            'w=1/(\s^2^(I)+0.0004I^2^)'
_refine_ls_hydrogen_treatment           ?
_refine_ls_shift/su_max                 0.0050
_refine_ls_shift/su_mean                0.0021
_refine_diff_density_max                0.44
_refine_diff_density_min                -0.24
_refine_ls_extinction_method
 'B-C type 1 Gaussian isotropic (Becker & Coppens, 1974)'
_refine_ls_extinction_coef              10400(500)
_refine_ls_abs_structure_details        ?
_refine_ls_abs_structure_Flack          ?
_refine_ls_abs_structure_Rogers         ?

loop_
 _atom_type_symbol
 _atom_type_scat_dispersion_real
 _atom_type_scat_dispersion_imag
 _atom_type_scat_source
 Ca  0.2262  0.3064
 'International Tables Vol C tables 4.2.6.8 and 6.1.1.1'
 P   0.1023  0.0942
 'International Tables Vol C tables 4.2.6.8 and 6.1.1.1'
 O   0.0106  0.0060
 'International Tables Vol C tables 4.2.6.8 and 6.1.1.1'
 F   0.0171  0.0103
 'International Tables Vol C tables 4.2.6.8 and 6.1.1.1'

_computing_data_collection ?
              _computing_cell_refinement ?
               _computing_data_reduction ?
           _computing_structure_solution ?
```

```
_computing_structure_refinement
 'Jana2006 (Petricek, Dusek & Palatinus, 2006)'
          _computing_molecular_graphics ?
_computing_publication_material
 'Jana2006 (Petricek, Dusek & Palatinus, 2006)'

#=============================================================================

# 8. ATOMIC COORDINATES AND DISPLACEMENT PARAMETERS

loop_
 _atom_site_label
 _atom_site_type_symbol
 _atom_site_fract_x
 _atom_site_fract_y
 _atom_site_fract_z
 _atom_site_adp_type
 _atom_site_U_iso_or_equiv
 _atom_site_symmetry_multiplicity
 _atom_site_occupancy
 _atom_site_calc_flag
 _atom_site_refinement_flags
 _atom_site_disorder_assembly
 _atom_site_disorder_group
  Ca1 Ca 0.333333 0.666667 0.00111(5) Uani 0.00774(16) 4 1 d . . .
  Ca2 Ca 0.24293(4) -0.00716(4) 0.25 Uani 0.00725(18) 6 1 d . . .
  P1 P 0.39852(6) 0.36890(6) 0.25 Uani 0.0057(2) 6 1 d . . .
  O1 O 0.32624(17) 0.48413(15) 0.25 Uani 0.0081(5) 6 1 d . . .
  O2 O 0.58796(17) 0.46605(16) 0.25 Uani 0.0109(5) 6 1 d . . .
  O3 O 0.34215(12) 0.25649(10) 0.07012(12) Uani 0.0129(4) 12 1 d . . .
  F F 0 0 0.25 Uiso 0.0101(8) 2 0.730(10) d . . .
  O4 O 0 0 0.305 Uiso 0.0101(8) 4 0.135(5) d . . .

loop_
 _atom_site_aniso_label
 _atom_site_aniso_type_symbol
 _atom_site_aniso_U_11
 _atom_site_aniso_U_22
 _atom_site_aniso_U_33
 _atom_site_aniso_U_12
 _atom_site_aniso_U_13
 _atom_site_aniso_U_23
 Ca1 Ca 0.0091(2) 0.0091(2) 0.0051(2) 0.00453(10) 0 0
 Ca2 Ca 0.0080(2) 0.0066(2) 0.0070(2) 0.00355(16) 0 0
 P1 P 0.0066(3) 0.0058(3) 0.0056(2) 0.00381(19) 0 0
 O1 O 0.0099(6) 0.0072(6) 0.0092(5) 0.0057(5) 0 0
 O2 O 0.0069(6) 0.0084(6) 0.0172(6) 0.0037(5) 0 0
 O3 O 0.0216(5) 0.0110(5) 0.0094(4) 0.0106(4) -0.0064(4) -0.0035(3)


#=============================================================================

# 9. MOLECULAR GEOMETRY


loop_
 _geom_bond_atom_site_label_1
```

```
 _geom_bond_atom_site_label_2
 _geom_bond_site_symmetry_1
 _geom_bond_site_symmetry_2
 _geom_bond_distance
 _geom_bond_publ_flag
  Ca1 O1 . . 2.3963(11) ?
  Ca1 O1 . 2_665 2.3963(9) ?
  Ca1 O1 . 3_565 2.3963(16) ?
  Ca1 O2 . 4_664 2.4466(13) ?
  Ca1 O2 . 5_564 2.4466(12) ?
  Ca1 O2 . 6_554 2.4466(15) ?
  Ca1 O3 . 7_665 2.7951(11) ?
  Ca1 O3 . 8_565 2.7951(16) ?
  Ca1 O3 . 9_555 2.7951(9) ?
  Ca2 O1 . 3_555 2.6813(17) ?
  Ca2 O2 . 2_655 2.3663(14) ?
  Ca2 O3 . . 2.4896(10) ?
  Ca2 O3 . 5_555 2.3436(10) ?
  Ca2 O3 . 8_555 2.3436(10) ?
  Ca2 O3 . 10_555 2.4896(10) ?
  Ca2 F . . 2.3102(4) ?
  Ca2 O4 . . 2.3409(4) ?
  Ca2 O4 . 10_555 2.3409(4) ?
  P1 O1 . . 1.5346(19) ?
  P1 O2 . . 1.5372(14) ?
  P1 O3 . . 1.5364(9) ?
  P1 O3 . 10_555 1.5364(9) ?
  O1 O1 . 2_665 2.906(2) ?
  O1 O1 . 3_565 2.906(3) ?
  O1 O2 . . 2.541(3) ?
  O1 O3 . . 2.5332(18) ?
  O1 O3 . 6_555 2.9485(13) ?
  O1 O3 . 9_555 2.9485(13) ?
  O1 O3 . 10_555 2.5332(18) ?
  O2 O3 . . 2.4830(12) ?
  O2 O3 . 3_665 2.9349(16) ?
  O2 O3 . 10_555 2.4830(12) ?
  O2 O3 . 12_665 2.9349(16) ?
  O3 O3 . 10_555 2.4730(12) ?
  F O4 . . 0.3781 ?
  F O4 . 10_555 0.3781 ?
  O4 O4 . 7_556 2.6808 ?
  O4 O4 . 10_555 0.7561 ?

loop_
 _geom_angle_atom_site_label_1
 _geom_angle_atom_site_label_2
 _geom_angle_atom_site_label_3
 _geom_angle_site_symmetry_1
 _geom_angle_site_symmetry_2
 _geom_angle_site_symmetry_3
 _geom_angle
 _geom_angle_publ_flag
  O1 Ca1 O1 . . 2_665 74.66(5) ?
  O1 Ca1 O1 . . 3_565 74.66(6) ?
  O1 Ca1 O2 . . 4_664 92.80(4) ?
  O1 Ca1 O2 . . 5_564 154.55(6) ?
```

```
O1 Ca1 O2 . . 6_554 124.00(4) ?
O1 Ca1 O3 . . 7_665 86.98(4) ?
O1 Ca1 O3 . . 8_565 142.26(4) ?
O1 Ca1 O3 . . 9_555 68.72(3) ?
O1 Ca1 O1 2_665 . 3_565 74.66(4) ?
O1 Ca1 O2 2_665 . 4_664 124.00(5) ?
O1 Ca1 O2 2_665 . 5_564 92.80(4) ?
O1 Ca1 O2 2_665 . 6_554 154.55(7) ?
O1 Ca1 O3 2_665 . 7_665 68.72(4) ?
O1 Ca1 O3 2_665 . 8_565 86.98(6) ?
O1 Ca1 O3 2_665 . 9_555 142.26(4) ?
O1 Ca1 O2 3_565 . 4_664 154.55(4) ?
O1 Ca1 O2 3_565 . 5_564 124.00(6) ?
O1 Ca1 O2 3_565 . 6_554 92.80(5) ?
O1 Ca1 O3 3_565 . 7_665 142.26(4) ?
O1 Ca1 O3 3_565 . 8_565 68.72(4) ?
O1 Ca1 O3 3_565 . 9_555 86.98(4) ?
O2 Ca1 O2 4_664 . 5_564 75.72(5) ?
O2 Ca1 O2 4_664 . 6_554 75.72(6) ?
O2 Ca1 O3 4_664 . 7_665 56.08(3) ?
O2 Ca1 O3 4_664 . 8_565 124.50(4) ?
O2 Ca1 O3 4_664 . 9_555 67.72(4) ?
O2 Ca1 O2 5_564 . 6_554 75.72(4) ?
O2 Ca1 O3 5_564 . 7_665 67.72(5) ?
O2 Ca1 O3 5_564 . 8_565 56.08(5) ?
O2 Ca1 O3 5_564 . 9_555 124.50(3) ?
O2 Ca1 O3 6_554 . 7_665 124.50(4) ?
O2 Ca1 O3 6_554 . 8_565 67.72(5) ?
O2 Ca1 O3 6_554 . 9_555 56.08(4) ?
O3 Ca1 O3 7_665 . 8_565 117.00(3) ?
O3 Ca1 O3 7_665 . 9_555 117.00(4) ?
O3 Ca1 O3 8_565 . 9_555 117.00(4) ?
O1 Ca2 O2 3_555 . 2_655 101.18(7) ?
O1 Ca2 O3 3_555 . . 149.49(2) ?
O1 Ca2 O3 3_555 . 5_555 71.50(4) ?
O1 Ca2 O3 3_555 . 8_555 71.50(4) ?
O1 Ca2 O3 3_555 . 10_555 149.49(2) ?
O1 Ca2 F 3_555 . . 106.53(5) ?
O1 Ca2 O4 3_555 . . 106.31(5) ?
O1 Ca2 O4 3_555 . 10_555 106.31(5) ?
O2 Ca2 O3 2_655 . . 74.32(5) ?
O2 Ca2 O3 2_655 . 5_555 86.04(3) ?
O2 Ca2 O3 2_655 . 8_555 86.04(3) ?
O2 Ca2 O3 2_655 . 10_555 74.32(5) ?
O2 Ca2 F 2_655 . . 152.29(6) ?
O2 Ca2 O4 2_655 . . 150.89(5) ?
O2 Ca2 O4 2_655 . 10_555 150.89(5) ?
O3 Ca2 O3 . . 5_555 136.53(4) ?
O3 Ca2 O3 . . 8_555 78.06(4) ?
O3 Ca2 O3 . . 10_555 59.56(3) ?
O3 Ca2 F . . . 81.71(3) ?
O3 Ca2 O4 . . . 86.44(3) ?
O3 Ca2 O4 . . 10_555 77.14(3) ?
O3 Ca2 O3 5_555 . 8_555 139.74(6) ?
O3 Ca2 O3 5_555 . 10_555 78.06(4) ?
O3 Ca2 F 5_555 . . 102.59(3) ?
O3 Ca2 O4 5_555 . . 93.64(3) ?
```

```
O3 Ca2 O4 5_555 . 10_555 111.51(3) ?
O3 Ca2 O3 8_555 . 10_555 136.53(4) ?
O3 Ca2 F 8_555 . . 102.59(3) ?
O3 Ca2 O4 8_555 . . 111.51(3) ?
O3 Ca2 O4 8_555 . 10_555 93.64(3) ?
O3 Ca2 F 10_555 . . 81.71(3) ?
O3 Ca2 O4 10_555 . . 77.14(3) ?
O3 Ca2 O4 10_555 . 10_555 86.44(3) ?
F Ca2 O4 . . . 9.2943(18) ?
F Ca2 O4 . . 10_555 9.2943(18) ?
O4 Ca2 O4 . . 10_555 18.589(4) ?
O1 P1 O2 . . . 111.62(8) ?
O1 P1 O3 . . . 111.15(6) ?
O1 P1 O3 . . 10_555 111.15(6) ?
O2 P1 O3 . . . 107.77(6) ?
O2 P1 O3 . . 10_555 107.77(6) ?
O3 P1 O3 . . 10_555 107.18(5) ?
Ca1 O1 Ca1 . . 10_555 91.11(5) ?
Ca1 O1 Ca2 . . 2_555 101.85(5) ?
Ca1 O1 P1 . . . 129.61(5) ?
Ca1 O1 O1 . . 2_665 52.67(3) ?
Ca1 O1 O1 . . 3_565 52.67(4) ?
Ca1 O1 O2 . . . 111.36(4) ?
Ca1 O1 O3 . . . 105.07(2) ?
Ca1 O1 O3 . . 6_555 126.65(8) ?
Ca1 O1 O3 . . 9_555 62.05(3) ?
Ca1 O1 O3 . . 10_555 163.13(6) ?
Ca1 O1 Ca2 10_555 . 2_555 101.85(5) ?
Ca1 O1 P1 10_555 . . 129.61(5) ?
Ca1 O1 O1 10_555 . 2_665 52.67(3) ?
Ca1 O1 O1 10_555 . 3_565 52.67(4) ?
Ca1 O1 O2 10_555 . . 111.36(4) ?
Ca1 O1 O3 10_555 . . 163.13(6) ?
Ca1 O1 O3 10_555 . 6_555 62.05(3) ?
Ca1 O1 O3 10_555 . 9_555 126.65(8) ?
Ca1 O1 O3 10_555 . 10_555 105.07(2) ?
Ca2 O1 P1 2_555 . . 97.38(5) ?
Ca2 O1 O1 2_555 . 2_665 137.06(8) ?
Ca2 O1 O1 2_555 . 3_565 77.06(5) ?
Ca2 O1 O2 2_555 . . 131.60(7) ?
Ca2 O1 O3 2_555 . . 79.77(4) ?
Ca2 O1 O3 2_555 . 6_555 48.92(3) ?
Ca2 O1 O3 2_555 . 9_555 48.92(3) ?
Ca2 O1 O3 2_555 . 10_555 79.77(4) ?
P1 O1 O1 . . 2_665 125.57(8) ?
P1 O1 O1 . . 3_565 174.43(7) ?
P1 O1 O3 . . 6_555 100.91(5) ?
P1 O1 O3 . . 9_555 100.91(5) ?
O1 O1 O1 2_665 . 3_565 60.00(5) ?
O1 O1 O2 2_665 . . 91.34(6) ?
O1 O1 O3 2_665 . . 135.41(5) ?
O1 O1 O3 2_665 . 6_555 114.14(5) ?
O1 O1 O3 2_665 . 9_555 114.14(5) ?
O1 O1 O3 2_665 . 10_555 135.41(5) ?
O1 O1 O2 3_565 . . 151.34(6) ?
O1 O1 O3 3_565 . . 142.47(5) ?
O1 O1 O3 3_565 . 6_555 75.50(5) ?
```

```
O1 O1 O3 3_565 . 9_555 75.50(5) ?
O1 O1 O3 3_565 . 10_555 142.47(5) ?
O2 O1 O3 . . . 58.60(5) ?
O2 O1 O3 . . 6_555 121.03(5) ?
O2 O1 O3 . . 9_555 121.03(5) ?
O2 O1 O3 . . 10_555 58.60(5) ?
O3 O1 O3 . . 6_555 109.75(5) ?
O3 O1 O3 . . 9_555 67.01(4) ?
O3 O1 O3 . . 10_555 58.43(5) ?
O3 O1 O3 6_555 . 9_555 96.54(5) ?
O3 O1 O3 6_555 . 10_555 67.01(4) ?
O3 O1 O3 9_555 . 10_555 109.75(5) ?
Ca1 O2 Ca1 4_665 . 7_665 89.74(6) ?
Ca1 O2 Ca2 4_665 . 3_665 113.77(4) ?
Ca1 O2 P1 4_665 . . 104.55(5) ?
Ca1 O2 O1 4_665 . . 125.45(4) ?
Ca1 O2 O3 4_665 . . 110.22(5) ?
Ca1 O2 O3 4_665 . 3_665 97.00(6) ?
Ca1 O2 O3 4_665 . 10_555 69.08(4) ?
Ca1 O2 O3 4_665 . 12_665 61.80(3) ?
Ca1 O2 Ca2 7_665 . 3_665 113.77(4) ?
Ca1 O2 P1 7_665 . . 104.55(5) ?
Ca1 O2 O1 7_665 . . 125.45(4) ?
Ca1 O2 O3 7_665 . . 69.08(4) ?
Ca1 O2 O3 7_665 . 3_665 61.80(3) ?
Ca1 O2 O3 7_665 . 10_555 110.22(5) ?
Ca1 O2 O3 7_665 . 12_665 97.00(6) ?
Ca2 O2 P1 3_665 . . 124.58(10) ?
Ca2 O2 O1 3_665 . . 90.42(7) ?
Ca2 O2 O3 3_665 . . 135.88(7) ?
Ca2 O2 O3 3_665 . 3_665 54.76(4) ?
Ca2 O2 O3 3_665 . 10_555 135.88(7) ?
Ca2 O2 O3 3_665 . 12_665 54.76(4) ?
P1 O2 O3 . . 3_665 154.63(3) ?
P1 O2 O3 . . 12_665 154.63(3) ?
O1 O2 O3 . . . 60.55(5) ?
O1 O2 O3 . . 3_665 134.74(6) ?
O1 O2 O3 . . 10_555 60.55(5) ?
O1 O2 O3 . . 12_665 134.74(6) ?
O3 O2 O3 . . 3_665 123.01(3) ?
O3 O2 O3 . . 10_555 59.73(4) ?
O3 O2 O3 . . 12_665 164.67(9) ?
O3 O2 O3 3_665 . 10_555 164.67(9) ?
O3 O2 O3 3_665 . 12_665 49.83(3) ?
O3 O2 O3 10_555 . 12_665 123.01(3) ?
Ca1 O3 Ca2 7_665 . . 99.26(4) ?
Ca1 O3 Ca2 7_665 . 6_554 99.96(4) ?
Ca1 O3 P1 7_665 . . 90.44(5) ?
Ca1 O3 O1 7_665 . . 112.52(4) ?
Ca1 O3 O1 7_665 . 5_554 49.23(3) ?
Ca1 O3 O2 7_665 . . 54.85(4) ?
Ca1 O3 O2 7_665 . 2_655 50.48(3) ?
Ca1 O3 O3 7_665 . 10_555 100.09(4) ?
Ca2 O3 Ca2 . . 6_554 117.89(3) ?
Ca2 O3 P1 . . . 96.33(4) ?
Ca2 O3 O1 . . . 116.29(4) ?
Ca2 O3 O1 . . 5_554 93.61(5) ?
```

```
  Ca2 O3 O2 . . . 106.01(5) ?
  Ca2 O3 O2 . . 2_655 50.92(3) ?
  Ca2 O3 O3 . . 10_555 60.22(3) ?
  Ca2 O3 P1 6_554 . . 141.62(7) ?
  Ca2 O3 O1 6_554 . . 109.21(5) ?
  Ca2 O3 O1 6_554 . 5_554 59.58(4) ?
  Ca2 O3 O2 6_554 . . 132.93(4) ?
  Ca2 O3 O2 6_554 . 2_655 131.30(5) ?
  Ca2 O3 O3 6_554 . 10_555 159.87(6) ?
  P1 O3 O1 . . 5_554 139.56(6) ?
  P1 O3 O2 . . 2_655 83.16(5) ?
  O1 O3 O1 . . 5_554 148.62(5) ?
  O1 O3 O2 . . . 60.86(6) ?
  O1 O3 O2 . . 2_655 117.54(5) ?
  O1 O3 O3 . . 10_555 60.78(4) ?
  O1 O3 O2 5_554 . . 103.53(5) ?
  O1 O3 O2 5_554 . 2_655 73.19(5) ?
  O1 O3 O3 5_554 . 10_555 138.27(7) ?
  O2 O3 O2 . . 2_655 66.72(6) ?
  O2 O3 O3 . . 10_555 60.13(3) ?
  O2 O3 O3 2_655 . 10_555 65.08(4) ?
  Ca2 F Ca2 . . 2_555 120.000(12) ?
  Ca2 F Ca2 . . 3_555 120.000(17) ?
  Ca2 F O4 . . . 90 ?
  Ca2 F O4 . . 10_555 90 ?
  Ca2 F Ca2 2_555 . 3_555 120.000(17) ?
  Ca2 F O4 2_555 . . 90 ?
  Ca2 F O4 2_555 . 10_555 90 ?
  Ca2 F O4 3_555 . . 90 ?
  Ca2 F O4 3_555 . 10_555 90 ?
  O4 F O4 . . 10_555 180.0(5) ?
  Ca2 O4 Ca2 . . 2_555 117.444(12) ?
  Ca2 O4 Ca2 . . 3_555 117.444(16) ?
  Ca2 O4 F . . . 80.7057(18) ?
  Ca2 O4 O4 . . 7_556 99.2943(18) ?
  Ca2 O4 O4 . . 10_555 80.7057(18) ?
  Ca2 O4 Ca2 2_555 . 3_555 117.444(16) ?
  Ca2 O4 F 2_555 . . 80.706(2) ?
  Ca2 O4 O4 2_555 . 7_556 99.294(2) ?
  Ca2 O4 O4 2_555 . 10_555 80.706(2) ?
  Ca2 O4 F 3_555 . . 80.7057(14) ?
  Ca2 O4 O4 3_555 . 7_556 99.2943(14) ?
  Ca2 O4 O4 3_555 . 10_555 80.7057(14) ?
  F O4 O4 . . 7_556 180.0(5) ?
  O4 O4 O4 7_556 . 10_555 180.0(5) ?

loop_
 _geom_torsion_atom_site_label_1
 _geom_torsion_atom_site_label_2
 _geom_torsion_atom_site_label_3
 _geom_torsion_atom_site_label_4
 _geom_torsion_site_symmetry_1
 _geom_torsion_site_symmetry_2
 _geom_torsion_site_symmetry_3
 _geom_torsion_site_symmetry_4
 _geom_torsion
 _geom_torsion_publ_flag
```

```
 ? ? ? ? ? ? ? ? ? ?

loop_
 _geom_hbond_atom_site_label_D
 _geom_hbond_atom_site_label_H
 _geom_hbond_atom_site_label_A
 _geom_hbond_site_symmetry_D
 _geom_hbond_site_symmetry_H
 _geom_hbond_site_symmetry_A
 _geom_hbond_distance_DH
 _geom_hbond_distance_HA
 _geom_hbond_distance_DA
 _geom_hbond_angle_DHA
 _geom_hbond_publ_flag
 ? ? ? ? ? ? ? ? ? ?


#===============================================================================

# 10. STRUCTURE-FACTOR LIST

loop_
 _refln_index_h
 _refln_index_k
 _refln_index_l
 _refln_F_squared_calc
 _refln_F_squared_meas
 _refln_F_squared_sigma
 _refln_observed_status
   0   1   0      305.34      274.66      2.02 o
  -1   2   0      149.98      124.18      0.88 o
   0   2   0      709.05      744.39      4.83 o
  -2   3   0      246.16      240.66      1.59 o
  -1   3   0     2233.10     2222.69     14.38 o
   0   3   0     3741.63     4284.56     26.36 o
  -3   4   0     3933.24     4429.70     28.90 o
  -2   4   0      116.88      122.32      1.07 o
  -1   4   0     1803.87     1890.17     12.05 o
   0   4   0      715.73      757.46      4.86 o
  -4   5   0     4021.05     4187.37     27.08 o
  -3   5   0     2268.85     2346.21     15.22 o
  -2   5   0       13.81       17.81      0.36 o
  -1   5   0     3617.99     3771.25     23.29 o
   0   5   0      280.23      269.13      1.96 o
  -5   6   0        0.56        5.04      0.36 o
  -4   6   0     3979.62     4066.38     28.81 o
  -3   6   0      821.05      902.13      6.46 o
  -2   6   0      251.59      234.79      1.96 o
  -1   6   0     1639.79     1708.85     12.22 o
   0   6   0      500.93      521.59      5.32 o
  -6   7   0     1746.48     1646.94     19.49 o
  -5   7   0     1218.74     1235.12     11.27 o
  -4   7   0       22.09       22.13      0.72 o
  -3   7   0      738.58      715.95      6.86 o
  -2   7   0     3864.82     3876.79     33.75 o
  -1   7   0     2205.24     2223.95     21.89 o
   0   7   0      107.66      130.68      2.69 o
```

-7	8	0	4201.03	4162.90	58.96	o
-6	8	0	526.60	538.58	8.70	o
-5	8	0	1293.89	1283.32	17.56	o
-4	8	0	3779.63	3817.13	51.49	o
-3	8	0	424.44	434.75	5.88	o
-2	8	0	66.11	61.46	1.80	o
-1	8	0	325.20	366.52	6.43	o
0	8	0	2717.51	2647.48	38.09	o
-8	9	0	11.51	21.77	1.44	o
-7	9	0	799.40	783.25	13.26	o
-6	9	0	118.19	114.36	3.23	o
-5	9	0	115.44	102.15	3.59	o
-4	9	0	153.58	165.38	4.13	o
-3	9	0	3.47	8.10	1.08	o
-2	9	0	1163.78	1143.97	17.36	o
-1	9	0	243.51	252.87	5.37	o
0	9	0	1198.19	1192.07	21.26	o
-9	10	0	634.80	606.07	11.74	o
-8	10	0	353.58	377.00	9.65	o
-7	10	0	141.11	143.23	7.36	o
-6	10	0	898.41	879.80	19.96	o
-5	10	0	1871.61	1859.17	39.59	o
-4	10	0	20.29	21.77	1.98	o
-3	10	0	1708.68	1637.00	35.08	o
-2	10	0	1270.63	1296.41	23.16	o
-1	10	0	307.61	292.59	6.62	o
0	10	0	486.04	470.82	9.63	o
-10	11	0	1852.70	1870.39	58.12	o
-9	11	0	1063.93	1058.78	34.77	o
-8	11	0	359.16	365.49	10.01	o
-7	11	0	1788.25	1824.25	39.29	o
-6	11	0	1463.35	1415.01	31.14	o
-5	11	0	102.23	98.99	4.13	o
-4	11	0	750.64	736.11	17.39	o
-3	11	0	12.20	18.54	2.16	o
-2	11	0	120.83	120.70	4.67	o
-1	11	0	104.52	109.78	3.77	o
0	11	0	16.79	27.35	2.52	o
-10	12	0	1020.24	1003.02	23.34	o
-9	12	0	330.85	345.41	9.84	o
-8	12	0	378.52	371.56	10.37	o
-7	12	0	23.08	25.37	2.52	o
-6	12	0	198.91	190.49	6.46	o
-5	12	0	943.19	953.92	22.12	o
-4	12	0	597.78	604.14	14.96	o
-3	12	0	1591.33	1635.53	35.69	o
-2	12	0	395.96	374.37	10.19	o
-1	12	0	29.06	33.46	2.70	o
0	1	1	139.65	152.36	0.88	o
-1	2	1	400.87	399.83	1.90	o
0	2	1	168.82	193.92	1.06	o
-2	3	1	2651.57	2704.72	12.15	o
-1	3	1	3555.53	3756.76	17.14	o
0	3	1	700.80	817.36	3.79	o
-3	4	1	972.44	981.71	4.44	o
-2	4	1	613.58	575.79	2.61	o
-1	4	1	488.94	591.56	2.81	o

0	4	1	67.10	67.29	0.54	o
-4	5	1	130.10	141.29	0.90	o
-3	5	1	2604.54	2655.18	12.15	o
-2	5	1	2699.32	2801.91	12.70	o
-1	5	1	260.27	262.57	1.43	o
0	5	1	894.41	980.93	4.87	o
-5	6	1	563.04	589.61	3.71	o
-4	6	1	1332.59	1349.87	7.03	o
-3	6	1	2209.37	2215.09	11.39	o
-2	6	1	335.14	346.08	1.96	o
-1	6	1	3486.80	3569.76	19.77	o
0	6	1	19.16	23.75	0.54	o
-6	7	1	544.76	548.46	4.61	o
-5	7	1	651.66	653.82	4.95	o
-4	7	1	102.37	111.08	1.08	o
-3	7	1	3210.30	3196.79	20.15	o
-2	7	1	1465.57	1433.48	10.50	o
-1	7	1	432.19	439.90	3.91	o
0	7	1	4.39	4.68	0.54	o
-7	8	1	4.95	3.42	0.54	o
-6	8	1	198.63	181.99	1.97	o
-5	8	1	6.08	8.82	0.54	o
-4	8	1	1131.18	1122.71	9.61	o
-3	8	1	158.64	156.33	1.79	o
-2	8	1	0.99	3.60	0.54	o
-1	8	1	140.90	143.17	1.79	o
0	8	1	48.92	53.40	1.26	o
-8	9	1	71.92	72.79	1.80	o
-7	9	1	6.87	9.72	0.90	o
-6	9	1	744.46	722.00	8.14	o
-5	9	1	899.15	894.95	8.46	o
-4	9	1	824.41	856.26	9.71	o
-3	9	1	2356.13	2277.15	24.17	o
-2	9	1	668.91	675.34	7.63	o
-1	9	1	128.28	141.28	2.69	o
0	9	1	629.96	607.05	7.64	o
-9	10	1	1.64	7.20	1.08	o
-8	10	1	580.62	596.02	8.90	o
-7	10	1	446.03	417.99	6.60	o
-6	10	1	1017.81	996.16	16.74	o
-5	10	1	599.11	581.21	10.49	o
-4	10	1	10.87	13.32	1.08	o
-3	10	1	848.73	896.01	12.74	o
-2	10	1	474.97	474.03	7.49	o
-1	10	1	329.13	316.28	5.01	o
0	10	1	195.50	184.39	3.77	o
-10	11	1	269.25	281.98	5.91	o
-9	11	1	1939.04	1923.93	29.17	o
-8	11	1	12.01	11.70	1.62	o
-7	11	1	3.30	5.58	1.44	o
-6	11	1	1217.63	1215.07	22.16	o
-5	11	1	918.82	893.41	14.50	o
-4	11	1	475.13	458.51	8.39	o
-3	11	1	249.21	262.32	4.84	o
-2	11	1	61.87	65.09	2.16	o
-1	11	1	2533.25	2510.47	33.50	o
0	11	1	56.23	62.58	2.88	o

-10	12	1	78.42	88.62	4.67	o
-9	12	1	528.26	569.13	11.95	o
-8	12	1	452.53	487.87	10.54	o
-7	12	1	335.81	377.55	8.59	o
-6	12	1	0.05	5.58	1.26	o
-5	12	1	370.85	382.86	7.51	o
-4	12	1	1.91	4.14	1.26	o
-3	12	1	136.15	135.76	3.77	o
-2	12	1	178.09	178.02	4.31	o
-1	12	1	6.59	12.96	2.70	o
0	0	2	2696.93	2678.06	31.56	o
0	1	2	1055.04	992.64	4.43	o
-1	2	2	3192.39	3165.34	15.53	o
0	2	2	2601.46	2586.05	13.73	o
-2	3	2	254.67	338.67	1.95	o
-1	3	2	928.15	1060.54	5.46	o
0	3	2	313.83	398.58	2.13	o
-3	4	2	2286.43	2397.06	11.50	o
-2	4	2	4754.08	4751.28	22.40	o
-1	4	2	1747.29	1761.39	8.58	o
0	4	2	3862.13	3780.31	19.17	o
-4	5	2	14.05	12.95	0.36	o
-3	5	2	140.48	144.13	0.90	o
-2	5	2	2919.99	2853.86	13.54	o
-1	5	2	337.86	351.15	1.96	o
0	5	2	4751.62	4573.92	28.80	o
-5	6	2	1165.57	1159.37	8.15	o
-4	6	2	366.66	398.14	3.02	o
-3	6	2	1026.93	1043.49	7.13	o
-2	6	2	522.84	519.12	3.54	o
-1	6	2	834.59	822.54	5.79	o
0	6	2	914.90	955.83	6.66	o
-6	7	2	773.03	731.04	5.64	o
-5	7	2	4481.90	4392.58	30.83	o
-4	7	2	2218.16	2165.52	16.66	o
-3	7	2	57.36	61.46	0.90	o
-2	7	2	857.35	884.25	6.85	o
-1	7	2	14.93	19.07	0.54	o
0	7	2	1343.61	1291.27	9.92	o
-7	8	2	437.63	433.79	3.92	o
-6	8	2	107.59	112.39	1.62	o
-5	8	2	3688.67	3569.86	27.94	o
-4	8	2	467.67	452.31	3.91	o
-3	8	2	3154.42	3109.00	24.12	o
-2	8	2	1439.02	1437.80	11.99	o
-1	8	2	1796.73	1752.66	15.01	o
0	8	2	4464.27	4366.58	35.47	o
-8	9	2	1769.33	1748.25	19.43	o
-7	9	2	66.76	60.40	1.44	o
-6	9	2	2436.08	2354.32	21.78	o
-5	9	2	593.47	602.98	5.51	o
-4	9	2	582.47	583.05	5.33	o
-3	9	2	1944.70	1957.84	17.91	o
-2	9	2	19.16	21.59	0.90	o
-1	9	2	114.26	114.40	1.98	o
0	9	2	399.30	409.03	5.54	o
-9	10	2	92.70	98.11	2.52	o

-8	10	2	1635.97	1614.21	20.57	o
-7	10	2	67.01	70.29	1.98	o
-6	10	2	34.82	37.41	1.26	o
-5	10	2	889.24	901.47	10.61	o
-4	10	2	124.33	118.87	2.87	o
-3	10	2	12.92	16.74	1.26	o
-2	10	2	213.16	205.80	3.76	o
-1	10	2	2.94	6.84	0.90	o
0	10	2	72.01	83.05	3.06	o
-10	11	2	40.30	48.39	2.16	o
-9	11	2	309.74	310.05	4.83	o
-8	11	2	354.19	334.63	5.72	o
-7	11	2	1.36	3.60	1.08	o
-6	11	2	70.57	73.70	2.70	o
-5	11	2	73.37	79.27	2.88	o
-4	11	2	133.42	140.78	3.41	o
-3	11	2	593.97	572.31	8.90	o
-2	11	2	312.26	318.27	5.55	o
-1	11	2	1813.72	1858.88	28.23	o
0	11	2	22.82	17.27	1.80	o
-10	12	2	12.45	14.76	2.16	o
-9	12	2	601.57	607.10	12.47	o
-8	12	2	1933.48	1942.13	34.42	o
-7	12	2	563.09	536.47	11.23	o
-6	12	2	718.14	717.33	14.22	o
-5	12	2	4.45	8.28	1.62	o
-4	12	2	1509.88	1465.09	22.96	o
-3	12	2	210.60	221.86	4.48	o
-2	12	2	63.40	65.45	3.96	o
0	1	3	87.00	112.89	0.72	o
-1	2	3	1229.20	1364.19	6.41	o
0	2	3	1115.77	1216.41	6.46	o
-2	3	3	3005.85	2963.89	14.37	o
-1	3	3	4835.98	4663.74	23.29	o
0	3	3	510.97	535.90	2.82	o
-3	4	3	846.62	844.54	4.53	o
-2	4	3	22.90	18.70	0.36	o
-1	4	3	1025.86	1047.84	5.53	o
0	4	3	25.84	23.02	0.36	o
-4	5	3	721.61	697.47	4.92	o
-3	5	3	391.95	365.47	2.84	o
-2	5	3	3207.20	3143.06	20.63	o
-1	5	3	591.01	563.85	4.06	o
0	5	3	178.46	171.52	1.61	o
-5	6	3	49.50	57.34	0.90	o
-4	6	3	2881.50	2774.74	20.65	o
-3	6	3	299.74	310.48	2.68	o
-2	6	3	247.46	241.82	2.32	o
-1	6	3	3240.28	3160.84	21.45	o
0	6	3	25.59	26.08	0.54	o
-6	7	3	501.43	486.53	4.27	o
-5	7	3	625.96	620.96	5.31	o
-4	7	3	12.88	14.58	0.54	o
-3	7	3	3907.72	3728.03	28.01	o
-2	7	3	1529.95	1487.04	11.59	o
-1	7	3	14.35	17.81	0.54	o
0	7	3	522.97	509.91	4.62	o

-7	8	3	268.00	251.63	2.68	o
-6	8	3	157.38	158.39	1.97	o
-5	8	3	0.59	1.26	0.36	o
-4	8	3	9.92	11.16	0.54	o
-3	8	3	243.66	248.28	2.51	o
-2	8	3	385.89	373.34	3.39	o
-1	8	3	23.26	25.91	0.72	o
0	8	3	79.97	78.71	1.62	o
-8	9	3	61.86	64.18	1.44	o
-7	9	3	141.82	143.23	2.33	o
-6	9	3	22.30	24.83	0.90	o
-5	9	3	547.66	540.07	5.34	o
-4	9	3	508.63	509.89	5.16	o
-3	9	3	974.57	936.17	9.17	o
-2	9	3	313.98	312.84	4.29	o
-1	9	3	87.33	90.03	1.80	o
0	9	3	692.57	673.89	10.13	o
-9	10	3	145.57	146.50	3.41	o
-8	10	3	661.50	683.99	8.71	o
-7	10	3	105.73	99.16	1.98	o
-6	10	3	514.44	521.50	5.70	o
-5	10	3	455.23	440.90	5.00	o
-4	10	3	3.69	5.76	0.72	o
-3	10	3	1613.94	1616.64	19.19	o
-2	10	3	697.77	702.00	9.06	o
-1	10	3	611.81	591.72	8.37	o
0	10	3	3.74	4.32	0.90	o
-10	11	3	531.89	522.95	10.88	o
-9	11	3	1650.95	1614.86	23.07	o
-8	11	3	11.87	16.38	1.26	o
-7	11	3	88.56	92.01	2.16	o
-6	11	3	426.64	425.11	5.72	o
-5	11	3	1146.98	1148.29	15.51	o
-4	11	3	338.34	341.37	6.08	o
-3	11	3	2.12	4.50	1.08	o
-2	11	3	287.59	303.75	5.73	o
-1	11	3	3263.26	3278.80	56.29	o
-9	12	3	428.08	453.88	9.65	o
-8	12	3	207.76	212.00	5.74	o
-7	12	3	27.45	36.88	2.52	o
-6	12	3	4.72	7.56	1.44	o
-5	12	3	6.70	11.88	1.44	o
-4	12	3	0.32	1.08	1.08	<
-3	12	3	109.66	116.06	5.03	o
0	0	4	5697.91	5547.90	79.56	o
0	1	4	312.35	333.39	1.78	o
-1	2	4	194.51	209.80	1.25	o
0	2	4	49.20	44.56	0.36	o
-2	3	4	1485.67	1520.15	7.84	o
-1	3	4	873.98	849.98	4.71	o
0	3	4	4172.83	3927.88	22.59	o
-3	4	4	126.73	121.21	1.26	o
-2	4	4	0.33	3.96	0.36	o
-1	4	4	232.62	233.22	1.79	o
0	4	4	376.79	373.61	2.85	o
-4	5	4	3595.20	3468.42	24.19	o
-3	5	4	979.14	929.20	6.82	o

-2	5	4	94.27	89.58	1.08	o
-1	5	4	2400.94	2325.77	16.73	o
0	5	4	943.54	907.40	6.84	o
-5	6	4	7.05	10.98	0.54	o
-4	6	4	2441.61	2372.36	17.50	o
-3	6	4	980.64	965.08	7.54	o
-2	6	4	1648.45	1612.07	12.06	o
-1	6	4	2409.24	2303.11	17.22	o
0	6	4	756.66	742.69	6.19	o
-6	7	4	2313.98	2162.50	17.21	o
-5	7	4	6.96	8.28	0.54	o
-4	7	4	67.76	72.43	1.08	o
-3	7	4	656.92	626.38	5.14	o
-2	7	4	1300.57	1287.22	10.12	o
-1	7	4	1299.34	1251.56	10.31	o
0	7	4	0.04	1.80	0.54	o
-7	8	4	3828.83	3670.80	33.38	o
-6	8	4	1204.62	1142.04	10.18	o
-5	8	4	860.63	829.64	7.42	o
-4	8	4	4057.60	3873.31	31.01	o
-3	8	4	459.14	446.00	4.46	o
-2	8	4	5.37	7.20	0.54	o
-1	8	4	220.48	221.68	3.05	o
0	8	4	1780.44	1733.16	17.19	o
-8	9	4	138.35	139.68	2.51	o
-7	9	4	425.48	429.58	4.64	o
-6	9	4	0.65	0.90	0.54	<
-5	9	4	30.75	29.32	0.90	o
-4	9	4	0.13	0.90	0.36	<
-3	9	4	54.70	55.20	1.26	o
-2	9	4	924.29	890.61	9.37	o
-1	9	4	56.74	57.54	1.44	o
0	9	4	728.76	721.36	8.70	o
-9	10	4	265.80	245.45	5.37	o
-8	10	4	86.13	91.66	1.80	o
-7	10	4	182.05	187.66	2.87	o
-6	10	4	488.18	470.06	5.17	o
-5	10	4	554.27	563.53	6.06	o
-4	10	4	95.43	94.87	1.62	o
-3	10	4	905.00	874.36	10.27	o
-2	10	4	874.57	886.96	10.45	o
-1	10	4	456.57	429.08	7.14	o
0	10	4	240.33	235.37	5.92	o
-9	11	4	1271.34	1216.71	27.11	o
-8	11	4	0.88	2.88	1.08	<
-7	11	4	1670.70	1672.93	19.39	o
-6	11	4	1017.65	1002.31	10.78	o
-5	11	4	230.49	229.47	3.59	o
-4	11	4	817.73	818.11	11.18	o
-3	11	4	0.42	0.00	1.08	<
-2	11	4	46.48	51.26	3.24	o
-8	12	4	390.85	402.15	10.37	o
-7	12	4	0.65	0.72	1.26	<
-6	12	4	201.30	198.76	9.15	o
-5	12	4	437.05	452.21	12.15	o
0	1	5	57.66	53.72	0.54	o
-1	2	5	301.75	277.75	1.78	o

0	2	5	214.36	197.48	1.43	o
-2	3	5	1566.18	1561.82	8.76	o
-1	3	5	3097.74	2991.16	16.78	o
0	3	5	129.36	131.83	1.08	o
-3	4	5	530.08	528.60	3.73	o
-2	4	5	480.45	443.39	3.38	o
-1	4	5	257.15	222.96	1.97	o
0	4	5	120.88	116.11	1.26	o
-4	5	5	38.32	38.84	0.72	o
-3	5	5	2009.54	1895.07	12.98	o
-2	5	5	1258.56	1250.09	9.59	o
-1	5	5	95.37	89.08	1.08	o
0	5	5	615.41	578.60	5.15	o
-5	6	5	420.93	416.77	3.75	o
-4	6	5	703.18	703.58	5.31	o
-3	6	5	1589.19	1524.91	11.27	o
-2	6	5	111.02	108.45	1.26	o
-1	6	5	2464.18	2368.06	20.72	o
0	6	5	13.42	13.86	0.72	o
-6	7	5	212.03	203.61	2.69	o
-5	7	5	428.26	404.79	3.92	o
-4	7	5	72.84	69.37	1.08	o
-3	7	5	1646.45	1576.36	13.02	o
-2	7	5	807.40	771.93	7.43	o
-1	7	5	326.54	318.82	3.58	o
0	7	5	26.43	29.68	1.08	o
-7	8	5	9.75	12.60	0.72	o
-6	8	5	114.70	111.17	1.62	o
-5	8	5	5.20	8.10	0.54	o
-4	8	5	875.74	851.69	7.78	o
-3	8	5	67.33	70.47	1.26	o
-2	8	5	29.18	31.30	0.90	o
-1	8	5	138.67	138.96	2.15	o
0	8	5	15.14	16.56	0.90	o
-8	9	5	60.76	68.51	1.80	o
-7	9	5	0.64	2.88	0.54	o
-6	9	5	743.14	727.19	6.57	o
-5	9	5	657.25	651.84	6.22	o
-4	9	5	603.89	600.88	6.05	o
-3	9	5	1770.69	1713.76	16.36	o
-2	9	5	534.97	549.39	6.24	o
-1	9	5	77.68	85.56	1.80	o
0	9	5	354.23	341.86	5.55	o
-9	10	5	1.17	1.80	0.90	<
-8	10	5	369.62	391.50	6.62	o
-7	10	5	412.74	412.27	5.90	o
-6	10	5	722.14	733.74	8.00	o
-5	10	5	410.15	392.42	4.65	o
-4	10	5	6.22	9.36	0.90	o
-3	10	5	434.38	433.72	6.61	o
-2	10	5	256.15	262.71	4.66	o
-1	10	5	167.08	163.69	5.56	o
-8	11	5	12.54	11.34	1.80	o
-7	11	5	0.23	2.34	0.72	o
-6	11	5	1087.90	1114.74	13.60	o
-5	11	5	615.11	607.70	8.01	o
-4	11	5	314.20	317.97	9.13	o

-3	11	5	215.34	237.63	10.58	o
0	0	6	7194.12	6704.87	77.93	o
0	1	6	549.70	550.09	3.37	o
-1	2	6	4116.38	3938.77	24.13	o
0	2	6	256.36	267.07	1.97	o
-2	3	6	257.59	249.04	1.97	o
-1	3	6	23.82	26.26	0.54	o
0	3	6	51.29	48.90	0.72	o
-3	4	6	2800.62	2685.56	17.65	o
-2	4	6	2973.51	2870.79	19.06	o
-1	4	6	17.07	19.79	0.54	o
0	4	6	1731.68	1672.79	11.76	o
-4	5	6	96.06	90.90	1.26	o
-3	5	6	1.41	1.80	0.36	o
-2	5	6	799.32	780.12	6.19	o
-1	5	6	435.94	428.74	4.10	o
0	5	6	1735.02	1669.22	15.61	o
-5	6	6	464.12	449.07	4.46	o
-4	6	6	508.81	501.31	4.28	o
-3	6	6	1394.64	1367.95	11.36	o
-2	6	6	60.96	55.55	1.08	o
-1	6	6	60.37	60.41	1.26	o
0	6	6	1372.02	1314.58	12.44	o
-6	7	6	88.59	87.33	1.62	o
-5	7	6	1122.40	1119.57	9.86	o
-4	7	6	651.55	649.46	5.87	o
-3	7	6	34.23	32.92	0.90	o
-2	7	6	82.53	83.93	1.44	o
-1	7	6	125.31	123.01	1.80	o
0	7	6	220.54	202.04	2.87	o
-7	8	6	53.34	57.19	1.62	o
-6	8	6	3.58	5.94	0.54	o
-5	8	6	2153.28	2104.36	17.27	o
-4	8	6	3.29	5.40	0.54	o
-3	8	6	1306.99	1277.35	12.47	o
-2	8	6	317.68	318.92	3.76	o
-1	8	6	1131.41	1103.05	12.70	o
0	8	6	3223.48	3208.39	38.81	o
-8	9	6	566.48	573.25	8.20	o
-7	9	6	2.25	3.96	0.90	o
-6	9	6	2478.26	2429.49	29.75	o
-5	9	6	189.13	188.19	2.87	o
-4	9	6	685.66	685.51	8.36	o
-3	9	6	1776.66	1712.73	20.22	o
-2	9	6	60.92	62.39	1.98	o
-1	9	6	783.68	790.91	10.83	o
-7	10	6	67.63	67.06	3.06	o
-6	10	6	22.01	23.39	1.26	o
-5	10	6	122.91	123.58	2.51	o
-4	10	6	405.88	417.57	7.87	o
-3	10	6	158.16	168.75	5.92	o
0	1	7	5.86	6.66	0.54	o
-1	2	7	0.49	1.62	0.36	o
0	2	7	8.15	10.26	0.54	o
-2	3	7	1270.68	1281.47	9.99	o
-1	3	7	2144.36	2134.96	17.18	o
0	3	7	79.83	80.87	1.26	o

-3	4	7	438.10	433.78	4.10	o
-2	4	7	166.09	163.62	1.79	o
-1	4	7	10.02	13.32	0.54	o
0	4	7	83.92	84.10	1.44	o
-4	5	7	137.26	134.47	1.80	o
-3	5	7	607.89	601.10	5.51	o
-2	5	7	1028.13	1027.97	9.35	o
-1	5	7	100.45	98.45	1.44	o
0	5	7	20.35	21.41	0.72	o
-5	6	7	212.96	218.57	2.51	o
-4	6	7	741.53	760.17	6.92	o
-3	6	7	603.20	599.63	5.70	o
-2	6	7	85.70	88.24	1.44	o
-1	6	7	1617.22	1608.75	14.32	o
0	6	7	12.28	14.58	0.72	o
-6	7	7	135.50	135.04	2.87	o
-5	7	7	336.78	331.19	4.29	o
-4	7	7	15.62	14.58	0.72	o
-3	7	7	1631.39	1611.97	13.97	o
-2	7	7	699.13	687.74	8.18	o
-1	7	7	136.04	128.75	2.51	o
0	7	7	36.84	40.29	1.44	o
-7	8	7	24.73	34.19	1.98	o
-6	8	7	95.11	102.61	2.52	o
-5	8	7	1.76	1.80	0.72	<
-4	8	7	189.47	191.61	3.41	o
-3	8	7	104.51	112.12	2.52	o
-2	8	7	15.03	14.76	1.08	o
-1	8	7	78.39	76.22	1.98	o
-6	9	7	202.41	194.99	9.33	o
-4	9	7	322.31	345.50	9.49	o
0	0	8	6911.62	6418.86	181.42	o
0	1	8	127.96	139.70	2.51	o
-1	2	8	96.33	102.77	1.98	o
0	2	8	21.42	24.11	0.90	o
-2	3	8	929.31	950.79	9.91	o
-1	3	8	408.90	417.48	4.47	o
0	3	8	1878.81	1903.10	17.19	o
-3	4	8	86.94	86.26	1.44	o
-2	4	8	0.68	0.90	0.54	<
-1	4	8	49.43	48.20	1.26	o
0	4	8	156.35	160.11	2.15	o
-4	5	8	1981.99	1997.18	21.18	o
-3	5	8	334.00	337.11	4.47	o
-2	5	8	42.15	48.56	1.26	o
-1	5	8	900.17	919.65	9.92	o
0	5	8	570.93	589.14	7.66	o
-5	6	8	48.28	50.18	1.62	o
-4	6	8	1173.39	1177.02	16.75	o
-3	6	8	486.59	504.20	7.32	o
-2	6	8	1403.73	1412.61	16.68	o
-1	6	8	1636.11	1653.55	19.23	o
0	6	8	465.79	477.49	7.86	o
-6	7	8	1478.70	1560.56	48.95	o
-5	7	8	53.97	65.82	5.04	o
-3	7	8	293.78	306.98	8.60	o
-2	7	8	372.40	405.83	10.73	o

0	1	9	7.80	8.10	1.44	o
-1	2	9	53.19	60.78	2.88	o
0	2	9	32.06	40.84	1.80	o
-2	3	9	792.71	831.02	10.47	o
-1	3	9	1797.72	1897.52	21.79	o
0	3	9	31.45	35.08	1.80	o
-3	4	9	191.50	214.76	4.84	o
-2	4	9	47.76	56.65	1.98	o
-1	4	9	150.97	164.10	3.05	o
0	4	9	30.37	35.08	1.62	o